R. & M. No. 3388

MINISTRY OF AVIATION

AERONAUTICAL RESEARCH COUNCIL
REPORTS AND MEMORANDA

The Effect of Forward Speed on the Inlet Flow Distribution and Performance of a Lifting Fan Installed in a Wing

By N. Gregory, M.A., W. G. Raymer, B.Sc.
and Edna M. Love

LONDON: HER MAJESTY'S STATIONERY OFFICE
1965
PRICE 16*s.* 6*d.* NET

The Effect of Forward Speed on the Inlet Flow Distribution and Performance of a Lifting Fan Installed in a Wing

By N. Gregory, M.A., W. G. Raymer, B.Sc.
and Edna M. Love

*Reports and Memoranda No. 3388**
June, 1962

Summary.

Five-tube yawmeter traverses immediately up and downstream of the fan reveal the flow maldistributions due to forward speed. These are removed by a deep duct or an inlet cascade, which turn the air into the axial direction. Non-uniformity of the exit static pressure, however, does not affect the flow distribution. Since forward speed reduces the pressure rise required, stalling of the fan blades appears not to be a great danger except at very high forward speeds, or when a deflected exit cascade is fitted.

1. *Introduction.*

Preliminary N.P.L. wind-tunnel tests on wings with submerged lifting fans have been described in a number of unpublished data reports by Gregory and Raymer[1, 2, 3]. Following this work, more detailed tests have been carried out on a new wing fitted with a more sophisticated fan unit. Some of the force data obtained have already been issued without detailed comment by way of example to Ref. 4: a fuller report is in course of preparation[11]. The present paper gives a description of the detailed flow measurements carried out just upstream and downstream of the fan and discusses the effect of forward speed on the flow distribution and on the overall fan performance. The modifications of the inlet flow distribution obtained by fitting an inlet cascade or by installing the fan much deeper in its duct (in a nacelle shaped fairing instead of a wing) are also described.

2. *Model Details and Experimental Arrangements.*

The model consisted of a symmetrical 15% thick rectangular wing with both chord and basic span of 64 in., plus wing-tip fairings of semi-circular cross-section. The aerofoil section was derived from NACA 0020 by adding a constant thickness region which extended over the chordwise length of the fan aperture. The model was fitted with a 20% plain flap and provided with split flaps which could be attached externally at 30° and 60° deflections. A general arrangement of the model, which was built by Messrs. Boulton Paul Aircraft Ltd., is shown in Fig. 1. A large number of pressure-plotting holes were also fitted.

The fan had a diameter, d, of 13·16 in. with a hub/diameter ratio of $\frac{1}{2}$ and was fitted in the wing with its axis normal to the chord line at 0·354 chord from the leading edge along the centre-line

* Replaces N.P.L. Aero. Report No. 1018—A.R.C. 23 839. Published with the permission of the Director, National Physical Laboratory.

of the model. The design of the fan is described in detail in the following section. The fan was located near the top of its duct, as is shown in Fig. 2, 2·6 in. or 20% duct diameter below the surface. The duct commenced with an inlet flare of lip radius 1·3 in. or 10% of the duct diameter. Except when the inlet cascade shown in Fig. 2a was in use, the fan hub was faired with a bluff boss with lip radius of 1 in., and the hub terminated immediately downstream of the stator-blade trailing-edge plane without any tail cone.

The fan was driven by a direct-current electric motor buried in the wing, *via* a 3/8 in. diameter extension shaft and bevel reduction gearing in the hub. The shaft crossed the annulus midway between two of the stator blades, and this was found to seriously disturb the flow through the fan (Section 5).

The fan hub boss and bottom plate were provided with fittings to locate rakes of three five-tube yawmeters which could be mounted either immediately upstream or downstream of the fan unit. The rakes could be rotated about the fan axis into any of 20 equally spaced positions by means of a hollow shaft which extended outside the tunnel and carried the pressure leads. The shaft was supported on a bearing at the hub of a tripod which was screwed to the surface of the wing. Means was provided for altering the radius of the probes, which were normally carried at 15, 50 and 85% of the annulus width, and for adjusting the angular position of the probes in each sector, which was normally midway between each pair of stator blades. The probes were kept aligned parallel to the axis of the fan and were used in this position, having previously been calibrated over a range of $\pm 30°$ by rotation of the probe arm about the appropriate axes when protruding through the wall into the working section of a 1 ft wind tunnel. The plane of the probe heads on the upstream side was 1·45 in. below the upper surface of the wing and 1·15 in. above the inlet guide vanes, and on the lower surface, 0·15 in. below the stator blades and 3·5 in. above the lower surface of the wing. Check traverses were also carried out with the probe heads in the plane of the lower surface of the wing. The traverses enabled estimations to be made of the mass flow through the fan and of the work done on the efflux by the fan. Electrical power input and torque measurements were not made.

The tests were carried out with the model suspended from the roof balance, first in the N.P.L. Duplex Wind Tunnel (14 ft × 7 ft), and following the demise of the tunnel in 1959, also in the 13 ft × 9 ft Wind Tunnel. The wing was the right way up with jet efflux directed towards the floor and the centre-line of the wing was 45·1 in. above the floor of the Duplex Wind Tunnel (0·54 × tunnel height) and 60 in. above the floor of the 13 ft × 9 ft Tunnel (0·55 × tunnel height). The plane of the duct exit in the lower surface was respectively 3·1 and 4·2 fan diameters above floor level in the two tunnels. Small differences therefore arose between the force measurements obtained in the two tunnels. These measurements are presented uncorrected for tunnel constraint, since appropriate corrections for models with lifting fans were not available. As pointed out by Wyatt[5], the corrections differ from those for a conventional model, and are more numerous.

3. *Fan Design.*

The fan was designed and constructed by Messrs. Armstrong Siddeley Motors Ltd. and had 20 inlet guide vanes with zero camber and outlet angles, a rotor with 21 blades and a stator with 20 blades, both with circular-arc aerofoils. The complete blading design is given in Table 1 which also gives the design performance specification.

It appears[6] that with a fan tip speed/jet velocity ratio of 1·69, the fan design is typical of the type of fan that has been considered for installation in a wing as a lifting fan. However, the design

stage adiabatic efficiency seems unduly low, and the blades (particularly the stator) are under-cambered by National Gas Turbine Establishment standards. Whilst this might curtail the operating range of the fan for pressure rises above the design value, owing to premature stalling of the blading, the experiments show that under forward-speed conditions the axial velocity through the fan is increased. Conditions in which this criticism of the fan design might prove important are when the fan is coping with severe maldistribution of flow, and when the pressure rise required of the fan is increased by reason of an exit cascade fitted to deflect the efflux.

4. *Fan Performance at Zero Forward Speed.*

As the fan was rigidly attached to the wing, the overall force measurements taken are of little use for assessing fan performance since, under forward-speed conditions, the measured lift increment on the wing due to operation of the fan is considerably affected by the interactions between the efflux and the mainstream resulting in substantial pressure changes over much of the wing. Also, both at forward speed and at rest, tunnel constraint seriously reduces the overall lift, due to the air entrained in the jet efflux creating suctions on the lower surface of the wing. This is clearly shown in Fig. 3 where the overall lift produced by the fan under static conditions has been plotted as a non-dimensional thrust coefficient $C_T(= L/\frac{1}{2}\rho A_F(\pi nd)^2)$, which is nearly independent of fan rotational speed except for a slight reduction at the lowest speeds due to the increasing importance of viscous effects. The measured values of C_T are roughly 25% below the design value of 0·706*. The values obtained in the 13 ft × 9 ft Wind Tunnel are slightly higher than those obtained in the Duplex Tunnel: this corresponds with the greater ground clearance in the 13 ft × 9 ft Tunnel. A big improvement in the Duplex Tunnel result was obtained by repeating the test with the floor boards removed. Although the joists, amounting to 28% of the floor area, remained in position, the jet diameter had increased to about 3 ft at floor level and streamed past several joists, so that recirculation of the jet and entrained air as a wall jet around the walls of the working section had practically ceased. Hence elimination of the joists does not seem likely to raise the thrust coefficient to its design value.

The flow through the fan (as explained below) is believed to be within 2% of its design value, so the remaining thrust deficiency must be due to suctions on the fan hub, the downstream end of which was cut off square without any streamline fairing. This conjecture was confirmed by adding a separately supported one-foot long cylindrical extension to the hub which thus protruded over eight inches below the lower surface of the wing so that the flow pattern downstream of the extension would not affect the forces developed on the wing. The gap between the hub and the extension was thus vented to local static, presumably close to ambient since the annulus was now of constant area. The lift rose by 77% of the deficit between its tunnel value without the extension and the design value, and the remaining 23% is accounted for by tunnel constraint. Attaching the extension to the hub on the other hand only increased the lift by 15% of the deficit: skin friction on the extension was now an additional debit whilst weak hub suctions were probably still present. A better result was obtained when a 5·2 in. long tail-cone fairing was added either directly to the hub, or to the end of the extension. This delayed the flow separation to about 2 in. from its apex and with either arrangement the lift was increased by about 25% of the deficit (Fig. 3).

---

* Since in the absence of interference and diffusion effects the static value of the lift is equal to $\rho A_F V_F^2$, the static value of the design fan thrust coefficient, C_T, should be equal to $2(V_F/\pi nd)^2$.

The hub tail-cone fairing was not used in the bulk of the work. Only a slight advantage was lost, since check measurements showed that the 7% improvement in lift (25% of the deficit) due to the use of the hub fairing was maintained at forward speeds but was accompanied by a 2% rise in drag increment due to the fan and also by an estimated rise in electrical power input also of about 2%. The change in power occurred since fitting the tail cone introduced a slight controlled diffusion of the efflux and consequent change in mass flow, thus altering the operating point on the fan characteristic.

A further complication in assessing fan performance and in correlating the force measurements with the flow traverses arose from the difficulty of estimating the mean flux through the fan from the limited number of readings taken. Although readings were taken at as many as 60 points, 3 points on each of 20 radii, the inner and outer points were at 15% and 85% of the annulus width, thus failing to record the regions of low velocity due to hub and duct boundary layers. Furthermore, on the exit traverses, the radii were in the middle of each sector thus recording the maximum velocity in each sector and failing to observe the region of lower velocity and the boundary layers on the stator blades. The nominal axial velocity deduced from the exit traverses thus appreciably exceeds the true flow, but the flow deduced from the inlet traverses where the velocities would not be expected to show any cyclic variation correlated with the downstream stator blading, and where the wall boundary layers would be thin (in the absence of appreciable separations) would be closer to the truth. The difficulty of assessing the true mean flow is perhaps emphasised by pointing out that the difference between the values calculated from the upstream and downstream traverses could be entirely accounted for, all other effects apart, by a change in boundary-layer displacement thickness on hub and duct walls of 0·1 in. thickness: in fact, boundary-layer growth probably accounts for about one quarter of the effect.

An estimate of the total-head rise characteristics of an identical fan has been obtained by Jager[7]. The flow rate through the fan was varied by altering the back pressure either by fitting gauze screens in a duct downstream of the fan or by discharging the flow into a region of reduced static pressure in a wind tunnel. The fan sucked in from still air, and velocity traverses were carried out immediately downstream of the fan. Non-dimensional representations of the fan characteristic suitable for the present purposes have been calculated from the Boulton Paul data and are shown in Fig. 4. The estimated flow under design conditions, $V_F/\pi nd$, is equal to 0·545 (less than the N.P.L. estimate of 0·582), and is less than the design figure of 0·596, and inconsistent with the measured thrust. This again serves to illustrate the difficulty of accurate measurement of fan flow rates.

5. *Inlet and Exit Flow Distributions.*

The flow directions measured just upstream and downstream of the fan can be presented in two ways, both of which are of interest. The yawmeter calibrations yield angles (θ, ϕ) relative to the traverse probe, where a positive value of ϕ represents a swirl in the direction of fan rotation and is important in relation to fan-blade-performance calculations, whilst positive θ represents an inflow towards the fan axis, and is of lesser importance. The flow direction can also be defined by the angles (α, β) measured from axes fixed in the model. Here positive α represents the deviation of the downward flow measured as a rotation from the vertical axis in the direction of the tail of the aircraft, and under forward-speed conditions is a measure of the inability of the influx to turn through 90° from the horizontal direction into the direction of the fan axis. On the other hand, β represents the less important deviation of the flow in a spanwise direction (to port, as viewed from above).

Traverses of the flow were undertaken just upstream and downstream of the fan with the plain circular inlet flare in position, the wing at zero incidence and fan rotational speed 41·7 rev/sec, at a number of forward speeds between zero and 50 ft/sec, and also with reduced fan rotational speeds at high forward speeds so as to obtain even larger values of the parameter V_T/V_F. At zero forward speed, and at very high forward speeds ($V_T/V_F > 0{\cdot}6$), the readings were found to be somewhat unsteady.

Circumferential distributions of the actual flow velocity (U) and directions (θ, ϕ) measured just upstream and downstream of the fan at zero, 30 and 50 ft/sec forward speeds are shown in Figs. 5 to 10, whilst the origins of the maldistributions which occur at forward speeds can be seen more clearly from Figs. 11 to 15, which show various contour plots of the velocity, static pressure, total head and flow deviations α and β obtained in some of the traverses. Total head has been measured as a departure from the mean total head in the plane of the traverse, and static pressure as a departure from the tunnel static pressure far upstream: both pressure differences have been rendered non-dimensional by dividing by the mean dynamic pressure of the flow through the fan.

The complete set of traverses reveal that at zero forward speed the upstream velocity rises slightly from hub to outer duct edge (Figs. 5, 11) and this is associated with the rather small inlet lip radius (0·10 duct diameter) which produces a suction peak associated with a local velocity 1·26 times the mean flow into the fan. The measured mean velocity 15% of the annulus gap from the wall is 1·12 times the mean velocity and an extrapolation of the radial distribution (ignoring the boundary layer) would lead to a value 1·20 at the wall. In fact, the adverse pressure on the wall just upstream of the fan is sufficient to provoke boundary-layer separation about $\frac{1}{2}$ in. ahead of the fan blade tips, and this was confirmed by the oil-flow techniques. The separated layer remains thin and the pressure rise through the fan causes reattachment of the flow. Neither upstream nor downstream of the fan was the outermost probe close enough to the duct wall to detect the boundary layer. The total head at entry is uniform and the static pressure varies over the annulus to match the velocity distribution. The fan exerts an appreciable smoothing effect on the flow. The flow velocity downstream of the fan is more nearly uniform over the annulus area (Fig. 6) except in the sector downstream of the drive shaft; here the flux is greatly reduced as the shaft creates locally stalled conditions. Magnus effect due to rotating shaft is also evident as the flow at a sector position of 250° is faster than that at the 290° position. The static-pressure variations from the mean are within $\pm 7\%$ of the dynamic pressure of the flow through the fan, or about $\frac{1}{4}$ of the variations on the upstream side, and the peak suctions are now measured nearest the hub and are associated with the flow expansion that takes place just below the plane of the traverse into the hub region, Fig. 2. The total-head variations also remain small at about $\pm 10\%$ of the dynamic pressure of the flow through the fan, but are of course much greater than the variations on the inlet side. The exit total head is least near the outside of the annulus, where the inlet velocity was highest. The exit traverse also reveals a few degrees of residual swirl which appears to indicate that the stator blades are under-cambered.

At increasing forward speeds, the separation from the upstream lip becomes more severe, whilst that over the rear half of the fan intake is eliminated. Oil-flow patterns obtained at a large value (0·55) of the forward speed ratio, V_T/V_F, revealed both long and short bubbles of separation with a torn vortex sheet as sketched in Figs. 16 and 17. The separated flow region still remained thin enough not to be detected by the traversing probe 0·5 in. from the wall.

The flow velocity into the fan had a considerable gradient from front to rear, Figs. 12a, 14a,

a speed ratio of 2:1 being observed at $V_T/V_F = 0{\cdot}55$, the high speeds being found at the front. Once again, the total-head distribution upstream of the fan was uniform, Fig. 12c*, and the static pressure varied to suit, Fig. 12b. The cyclic variations of θ and ϕ (Figs. 7, 9) imply only a small flow deviation in the spanwise direction, Fig. 12e, where this is seen to be a consequence of hub and duct curvature, but a considerable deviation of the flow towards the rear. In fact Figs. 12d and 14b show that the flow is in the axial direction only at the back of each part of the annulus where the duct walls control it. Maximum rearward inclinations of the flow are observed on the sides of the hub where the vertical walls exert their least effect. Fig. 18 shows how the mean values of α and β vary with forward-speed ratio up to $0{\cdot}55$: traverses at higher speed ratios could not be evaluated as the flow angles exceeded the range of calibration of the yawmeter probes. The curve $V_T/V_F = \tan\alpha$ would apply to fluid that conserves its horizontal momentum from far upstream. Thus it can be seen that the air entering the fan still possesses some $\frac{2}{3}$ of its horizontal momentum. The implication of this cross flow is that the retreating blade is subjected to a larger local angle of attack than the advancing blade, though this is to some extent relieved by the somewhat greater velocities found on the advancing side of the fan as seen in Figs. 12a and 14a. Nevertheless, the maldistribution shown by Figs. 12a to e implies a severe cyclic loading of the fan, which, whilst acceptable in these tests might lead to structural and vibration difficulties at full-scale. The improvements that can be achieved in this respect by turning vanes and depth of duct are discussed in Sections 7 and 8. A further technique for improvement, which is to be investigated in further experiments, is to tilt the fan axis forward by, say, 15°. At this angle, conservation of all the momentum should yield mean axial flow at a forward-speed ratio of $0{\cdot}26$, or even at $0{\cdot}41$ if only $\frac{2}{3}$ of the momentum is found at plane of the traverse.

Immediately downstream of the fan, on the other hand, the flow variations are all seen to be somewhat less than upstream, if the drive-shaft sector is ignored. The flow directions are relatively close to the axial (Figs. 8, 10). The flow velocities now increase from front to rear of the fan (Figs. 13a, 15a) as might be expected from the fact that the flow into the fan is moving towards the rear of the duct, and apart from the situation being obscured by the influence of the driving shaft, the flux on the advancing side of the duct can be seen still to be greater than that on the side where the rotor blades are retreating. As at zero forward speed the static pressure on the exit side of the fan is reasonably constant, though high at the front of the duct and low close to the hub. The regions of high velocity at exit from the fan, however, now possess high total head.

It is also interesting to note that although the exit traverse was carried out at a distance only $0{\cdot}25$ duct diameter away from the wing surface, up inside the duct, Fig. 2, the static-pressure suction peaks observed round the duct exit due to the interaction between the efflux and the mainstream could not be seen in the plane of the exit traverse though they were present when the

* The contours of Fig. 12c are drawn at one-fifth the intervals of those of static-pressure variation Fig. 12b, or of those of total-head or static-pressure variation (Figs. 13b, c) on the exit side. The mean total head of Fig. 12c implies a loss of total head from the value far upstream in the tunnel, of $1\frac{1}{2}\%$ of the mean dynamic pressure in the fan duct (or 13% of the tunnel dynamic pressure). The regions in the middle of the annulus where total head exceeds the mean value also include regions where the total head is up to $1\frac{1}{2}\%$ greater than the value far upstream. This seems unlikely and it suggests that the yawmeter was inadequately calibrated when yaw and pitch were both present. The total-head readings therefore cannot be relied on to within 2% of local dynamic pressure, which at V_T/V_F of $0{\cdot}33$ is not better than 20% of the dynamic pressure due to forward motion.

traverse was repeated in the plane of the lower surface, in which situation the flow was found to be somewhat unsteady, probably on account of the separation from the hub. The pair of traverses referred to were carried out at a different forward speed and so are not presented here. It may be suggested that previous reports have possibly overemphasised the magnitude of the suctions observed at forward speed round the jet exit. When non-dimensionalised in terms of the dynamic pressure of the efflux, as here, rather than in terms of that of the mainstream, the analysis of previous work[2, 8] suggests that at a V_T/V_F of 0·33 as in Fig. 13b, a high pressure coefficient of about +0·04 would be found at the upstream edge of the duct, a lesser value of about −0·2 at the downstream edge, and the marked suction peaks, which are only about −0·55 at angular positions ±140° round from the upwind generator. The range of variation falls off rapidly with distance away from the duct edge, both towards and away from the duct axis. Although pressure variations of this order can be seen in Fig. 13b, the distribution up inside the duct is not associated with the cyclic variation found in the external field but only with the increased static pressure on the front edge of the duct. Traverses immediately downstream of the fan at still higher forward speeds show that this region of increased pressure leads to flow separation immediately downstream of the fan at $V_T/V_F = 0{\cdot}8$. Such a speed ratio would only occur during the starting and shutting down of the fan in wing-borne flight.

Further traverses immediately downstream of the fan carried out at the (still high) forward-speed ratio of 0·42 show that the efflux distribution is substantially unaffected by wing incidence over the range ±12°, or by presence of 30° of split flap. It must be remembered, however, that the fan diameter is only a small fraction of the wing chord.

6. *Effect of Forward Speed on Fan Performance.*

The mean flow rate through the fan has been estimated from the traverses, and its variation with forward speed, both quantities non-dimensionalised in terms of the fan-blade-tip speed, is shown in Fig. 19. This graph again illustrates the difficulty referred to earlier that the flow rate is overestimated by the observations of the exit traverses. The small effects of incidence and presence of 30° split-flap deflection on the flow through the fan is also seen in Fig. 19.

The flow rate through the fan increases at first with forward speed, but with increasing maldistribution this tendency is reversed. The mean pressure rise across the fan was calculated from the upstream and downstream traverses and this allowed the effect of the maldistribution on the fan performance to be shown in Fig. 20. The characteristic in uniform flow is that shown in Fig. 4 and as explained earlier probably suffers from an overestimate of the flow. The flow rate in the N.P.L. measured characteristic was obtained from the inlet traverses, and the displacement in the zero forward-speed point from the design point can in part be associated with a reduction in V_F due to the blockage of one sector with the drive shaft, and to an even larger reduction in head rise which the fan has to supply on account of the slight increase in efficiency due to some diffusion of the flow between fan exit and duct exit.

With increasing forward speed the N.P.L. measured characteristic runs parallel with the characteristic for uniform inflow, but above a forward speed ratio, V_T/V_F of about 0·3, the maldistribution results in a deterioration in fan performance. The pressure rise demanded of the fan decreases with forward speed and the fan appears to be free from stalled flow regions at least as far as a forward-speed ratio of 0·55. As only one point of the complete fan characteristic was measured at any forward-speed ratio, it is not possible to say that the fan operating point is moving

away from the stall point, since this itself may be reduced and modified by severe cross-flow conditions. Further comments on the pressure rise through the fan are made in the companion paper[11].

The measured total-head rise $\Delta H/\frac{1}{2}\rho V_F^2$ of Fig. 20 includes an entry loss measured as 0·002 at V_T/V_F equal to 0·16, 0·015 at 0·33, 0·019 at 0·44 and 0·06 at 0·55, but as explained in an earlier footnote some of this may be fictitious and due to inadequate yawmeter calibration.

Power input to the fan was not measured.

7. *Effect of an Inlet Cascade.*

Tests were carried out with a variety of settings of the crude cascade of flat-plate vanes shown in Figs. 2 and 21. This cascade has the advantage of being able to seal off the duct for conventional forward flight. In the preliminary work the blades were ganged together so as all to have the same setting, and the cascade was tried both with and without the vertically aligned rear half of each blade. Measurement at a given fan rotational speed revealed at each value of the forward speed an optimum but rather ill-defined setting of the blades for maximum lift increment due to the fan. The blade angle with the vertical increased from 0° at zero forward speed to about 40° at 40 ft/sec ($V_T/V_F = 0{\cdot}44$). The effects on lift were small, and only between V_T/V_F values of 0·33 and 0·44 was the optimum result with the cascade present better than that obtained without the cascade. This was mostly due to the low Reynolds number since tests at zero forward speed showed that the skin friction on the lower vertical half of each blade diminished the lift by 4·5%, and addition of the upper halves, even with an individual setting for each blade*, reduced the lift by about another 2·2% (estimated). Hence an improvement of momentum flux of over 7% would be required in these model tests before an increase in lift would be measured.

Further steps were taken to improve the flow by adopting a differential setting for the blades, as in Refs. 9 and 10. Adjustments to the individual settings were made on the evidence of threads in indicating flow separations, force measurements and yawmeter traverses. At a number of yawmeter-probe positions, however, the probe was found to lie in the wake of a blade and the readings had to be discarded.

In the final configuration, Figs. 2 and 21, the first two blades were cambered to match the radius of the intake flare so that they could be used satisfactorily at large angle settings, and the tips of the first four blades were curved in planform in order to avoid a local stalling of the flow. At the rear of the cascade the top half of the penultimate blade and the whole of the last blade were eliminated as flow guidance was not required there.

At a forward speed of 40 ft/sec (V_T/V_F equal to 0·44) the optimum setting of the cascade blades was as depicted in Fig. 22 which also shows the variation from front to back of the duct of the underturning angle, $\alpha°$, meaned over the area of each blade, both with and without the cascade. The flow velocity distributions are compared in Fig. 23 and a contour plot of the velocity is given in Fig. 24. The effectiveness of the cascade in turning the flow into the axial direction has eliminated the cyclic variation in velocity observed without it. The increase in velocity towards the outer edge of the duct was also found without the cascade at zero forward speed, Fig. 11.

* This refers to the suggestion of Gilmore and Graham[9] that even at zero forward speed only the vanes in the vicinity of the fan axis should be set at 0°, those towards the front of the duct should face forwards and those at the back, to the rear. Negative blade settings were not possible with the present cascade, but when the front four blades were individually adjusted to settings of 62°, 30°, 15° and 5° so that flow separation (as indicated by threads) was altogether avoided, a 1·7% gain in lift was obtained over that with the 0° setting for all blades.

The forward speeds at which it would be necessary to alter the setting of the cascade in order to maintain reasonably axial flow could not be determined from the limited traverses that were taken, although it was observed that a change of forward speed of 10 ft/sec with the cascade setting of Fig. 22 altered the mean flow angle by less than a degree. It would be expected that the speed range for a given setting would be extended by the use of round-nosed blades with some thickness but further work would be required to confirm the contention[9] that transition could be carried out with only two settings of a cascade, one for hovering and another optimised for a forward speed in the upper half of the transition speed range.

It was not possible to show that an improved point on the fan operating characteristic (Fig. 20) was obtained by the use of the cascade at forward speed since so many readings had to be discarded that no reliable estimate of either mean incoming total head or flow rate could be made. In between the blade wakes, the total head measured was equal to that far upstream, and the flow velocities of Figs. 23 and 24 (which were in excess of those measured without the cascade) ignored the local regions of low velocity wakes.

8. *On the Influence of Duct Length.*

Some traverses were carried out immediately downstream of the fan with various duct extensions in position, either upstream or downstream of the fan. Whilst the addition of a duct 1·25 diameters in length upstream of the fan reduced the flow through the fan at zero forward speed, it was found that the addition of a 1·67 diameter-length downstream extension increased the flow at constant rotational fan speed by about 10%. This must be because the added length of duct allowed better diffusion of the flow downstream of the hub. At 30 ft/sec forward speed ($V_T/V_F = 0{\cdot}33$), however, without any duct extensions, it was established that the 23% change in flow speed between duct wall and hub measured along the upwind radius immediately below the fan (Figs. 8, 13a) was due to the non-uniform conditions at entry since when the 1·25 diameter length of entry duct was fitted, which extended to outside the wind tunnel, a uniform velocity distribution was found immediately below the fan despite the proximity of the lower surface of the wing and associated pressure field. When the fan was exposed to the cross-flow at entry, resulting in the upstream flow distribution of Figs. 7 and 12a, the duct extension 1·67 diameters in length below the fan reduced the 23% variation in speed to 9%.

It is not necessary, however, to avoid cross-flow at the duct inlet altogether in order to improve the flow distribution immediately upstream of the fan. The fan and a second identical fan have now been installed in tandem in a deep nacelle-shaped body. This has allowed a one-diameter length of duct both upstream and downstream of the fan. A streamlined hub boss and tail cone whose nose and tail are well within the overall depth allow acceleration of the flow into the fan and diffusion downstream. The lip radius has been increased from the present 0·10 duct diameter to a value that changes continuously between 0·23 diameter at the front of the duct and 0·11 diameter at the rear. In consequence, separation of the flow is avoided at forward speeds below 25 ft/sec ($V_T/V_F = 0{\cdot}28$). At the high forward speed of 50 ft/sec ($V_T/V_F = 0{\cdot}55$) the distribution of velocity and underturning angle immediately upstream of the fan are as shown in Figs. 25a and b which can be compared with Figs. 14a and b. Fig. 25 was obtained with both fans rotating, but this does not affect the comparison. It will be seen that the velocity distribution and flow underturning are very much improved although the extra length of duct between entry lip and fan has allowed the separated flow region to extend considerably. The negative flow angles recorded at the front indicate flow towards the wall following collapse of the bubble. Note also that the region of fastest flow is now found at the middle of the duct.

An available semi-circular piece of cambered slat was fitted in the forward half of the duct at the entry in an attempt to prevent boundary-layer separation. The slat used was successful up to a forward speed of 35 ft/sec ($V_T/V_F = 0{\cdot}39$) and even at higher forward speeds, the flow was much improved. Figs. 26a and b show the distribution at 50 ft/sec ($V_T/V_F = 0{\cdot}55$) and can be compared with Figs. 25a and b.

9. *Effect of an Exit Cascade.*

A number of force measurements and very few traverses were carried out with a simple cascade of 12 hinged flat-plate blades fitted to the lower surface across the duct in order to deflect the jet aft. This cascade was also capable of closing off the duct when the fan was shut down. The interest lay principally in the effect of jet deflection on the aerodynamic interactions.

As would be expected from the discussion so far, any alteration that occurred in the static-pressure distribution just upstream of the cascades due to their introduction did not appreciably affect the velocity distribution immediately downstream of the fan. More serious was the fact that the operating point on the fan characteristic was raised on account of the additional pressure drop suffered by the flow in traversing the deflected cascade. With the cascade blades all hinged in the plane of the lower surface, the cross-sectional area available for the flow was reduced by the factor $\cos\theta$ where θ was the deflection angle of the jet, quite apart from the effect of viscous losses due to the blades themselves. At 30 ft/sec forward speed (or V_T/V_F approximately $0{\cdot}37$) the value of $\Delta H/\frac{1}{2}\rho V_F^2$ was raised from $0{\cdot}675$ without the cascade to $1{\cdot}01$ with the cascade present and deflected 30° (Fig. 20). However, the reduced flow rate, $V_F/\pi nd$, of $0{\cdot}56$ remained well above the stalling value in uniform flow of $0{\cdot}43$ (Fig. 4), but the plotted point shows that maldistribution of the flow was still present and spoiling the fan performance.

The force measurements, coupled with output-power estimates (for both fan and assumed thrust unit)[4], suggested that very little was to be gained by exit-cascade deflection, and that 20° represented the optimum deflection at the lower forward speeds where the interaction effects were adverse. The lift and drag increments due to the fan fell increasingly short of the theoretical predictions as the flap deflection increased beyond 30°, but in the absence of flow-rate measurements it was not possible to determine for certain under what conditions the fan became stalled. Improvements were sought by deflecting only the rear half of the jet, and alternatively, by separating the cascade from the lower surface by 2 in. ($h/d = 0{\cdot}15$). Both these expedients reduced the drop in flow and change in pressure rise by about one-half of that caused by the plain 30° cascade, but the effects of maldistribution persisted. Both modifications reduced the thrust obtainable by the given cascade setting, but were offset by a smaller loss in lift. On balance, the half-cascade deflection slightly reduced the overall output-power level, whilst the separated cascade yielded a small reduction only at high forward speeds.

10. *Drive Shaft and Gas-Feed-Pipe Interference.*

The adverse influence of the mechanical drive shaft on the flow distribution on the exit side of the fan is amply illustrated by the figures of this paper. An alternative method of driving a fan is by means of a hub turbine using hot or cold gases generated remotely. This will require sophisticated streamline ducting to convey the gases across the annulus to the hub, since a plane circular cylinder of appropriate diameter ($4\frac{1}{2}$ in.) spanning the fan entry with its downstream generator in the plane of the leading edge of the fan stator blades can be seen to have disastrous effects on fan performance, Fig. 3.

Under static conditions, the thrust of the fan was reduced to about 46% of its normal value at the same rotational speed, and under forward-speed conditions a corresponding performance was obtained. The reduction in static thrust was much larger than could be accounted for by any calculation based on blockage of the duct or drag of the cylinder. Downstream traverses revealed that the flow was extremely unsteady, and that a large portion of the fan was stalled: there was no flow at all through a number of sectors below the feed pipe, and the axial velocity in the sectors rose only slowly with angular displacement from the feed pipe, reaching a maximum of 90% of the flow velocity in the absence of the feed pipe only in the sectors on the diameter at right angles to that occupied by the feed pipe.

11. *Conclusions.*

The flow traverses that have been carried out immediately upstream of the fan have revealed that with the fan situated just below the inlet flare, the observed maldistribution at forward speeds arises from incomplete turning of the flow into the duct. Submerging the fan one duct diameter below the entry largely eliminates the underturning of the flow, though at the expense of increasing the adverse effects of any flow separation on the inlet flare.

In this respect an inlet flare radius of 0·10 duct diameter gave rise to flow separation, even under zero-forward-speed conditions. A radius 0·23 duct diameter at the front of the duct eliminated flow separation up to a forward speed 0·28 times the speed through the fan, and a simple slat to control the boundary layer raised the maximum speed without separation to 0·39 times the speed through the fan. Slat design refinements or other means of boundary-layer control, coupled with consideration of hub shape and location could probably improve on these figures.

A crude form of inlet cascade with articulated flat-plate blading also satisfactorily reduced the flow divergences from the axial direction, but at model scale, the benefits of improved flow were nullified by the drag of the cascade which was 7% of the installed thrust. There is scope for a refined design of inlet cascade, coupled with tests at much higher Reynolds numbers.

Since about $\frac{2}{3}$ the horizontal momentum was still present in the fan entry, measured immediately below the inlet flare, tests are desirable with an inclined fan axis. 15° forward tilt should then yield truly axial flow at a forward-speed ratio of 0·4. Hence reasonable flow might be expected without a cascade over a large speed range. Such tests will be carried out as part of the fan-in-nacelle programme.

On the exit side of the fan, the pressure variations arising from the interactions between the efflux and the mainstream have very little upstream influence. Suction peaks could not be found even 0·25 duct diameter up inside the duct, and the pressure peak only provoked flow separation at the fan at very high forward speeds. With a limited depth of duct, the fan should be placed close to the bottom. If a long duct is available further tests are required to establish a compromise position which would allow a streamlined hub tail cone to be fitted and permit efficient diffusion of the flow in the downstream portion of duct.

Under forward-speed conditions the operating point on the fan characteristic moves away from the stall point in axial flow, and even with the worst cross-flow conditions (i.e. the fan close to the upper surface and without any entry cascade) the pressure rise through the fan is not adversely affected by cross-flow below a forward-speed ratio of about 0·25. Care should be taken in installing an exit cascade as this will increase the pressure rise demanded of the fan. For practical application, the use of variable-pitch blading to maintain constant fan speed operation should be considered.

NOTATION

ρ	Density
A_F	Annulus area
A_W	Wing area
r	Radius
d	Fan or duct diameter
L	Lift, including force produced by fan
n	Fan rotational speed, rev/sec
C_T	Fan force coefficient $\{= L/\frac{1}{2}\rho A_F(\pi nd)^2\}$
U	Flow velocity in fan
V_F	Axial component of flow velocity through fan
V_T	Forward speed
p	Static pressure
p_T	Reference static pressure far upstream
H	Total head
ΔH	Total-head rise across fan disc
θ	Inflow angle, i.e. deviation of flow from the axial direction towards the fan axis, or $\tan^{-1}(V_R/V_F)$ where V_R is the inward radial component of flow velocity
ϕ	Swirl angle, i.e. deviation of flow from the axial direction in the direction of fan rotation, or $\tan^{-1}(V_\phi/V_F)$ where V_ϕ is the tangential component of flow velocity
α	Underturning angle, i.e. deviation of flow from the axial direction towards the rear, or $\tan^{-1}(V_X/V_F)$ where V_X is the chordwise component of flow velocity
β	Spanwise flow angle, i.e. deviation of flow from the axial direction towards the port wing tip, or $\tan^{-1}(V_Y/V_F)$ where V_Y is the spanwise component of flow velocity.

REFERENCES

No.	*Author(s)*	*Title, etc.*
1	N. Gregory and W. G. Raymer . .	Wind tunnel tests on the Boulton-Paul rectangular wing (aspect ratio 2) with lifting fan—Series I. A.R.C. 20,356. August, 1958.
2	N. Gregory and W. G. Raymer . .	Wind tunnel tests on the Boulton-Paul rectangular wing (aspect ratio 2) with lifting fan—Series II. A.R.C. 21,127. July, 1959.
3	N. Gregory and W. G. Raymer . .	Wind tunnel tests on the effects of the apex fan on a swept wing project for V.T.O.L. with three lifting fans. A.R.C. 21,260. September, 1959.
4	N. Gregory	On the representation of fan-wing characteristics in a form suitable for the analysis of transition motions, with results of tests of an aspect-ratio-1 wing with fan at 0·354 chord. A.R.C. C.P. 552. August, 1959.
5	L. A. Wyatt	Preliminary note on wind-tunnel tests of a wing fitted with multiple lifting-fans. R.A.E. Tech. Note Aero. 2643. A.R.C. 21,377. October, 1959.
6	R. P. Bonham	Private Communication.
7	D. G. Jager	To determine the flow-rate characteristics of a 13·16 in. diameter fan. Boulton Paul Aircraft Ltd., Tech. Note 14. August, 1959.
8	—	A note on the aerodynamics of a wing-fan system. Boulton Paul Aircraft Ltd., Tech. Note 2. A.R.C. 19,890. February, 1958.
9	A. W. Gilmore and W. E. Grahame	Research studies on a ducted fan equipped with turning vanes. Inst. Aero. Sci. Report 59–59, 27th Ann. Mtg., New York. 26th January, 1959.
10	D. H. Hickey and D. R. Ellis . .	Wind-tunnel tests of a semispan wing with a fan rotating in the plane of the wing. NASA Tech. Note D–88. October, 1959.
11	N. Gregory, W. G. Raymer and E. M. Love	Wind-tunnel tests of a wing fitted with a single lifting fan. Report in preparation.

TABLE 1

Fan-Blading Design and Performance Specification
Free-Vortex Design

	$2r/d$	α_1	α_2	ϵ	$(S/c)_N$	$(S/c)_A$	α_1'	α_2'	θ	ξ	δ	c	N
Rotor	1·0	59·2	52·4	6·8	3·2	1·57	59·2	48·2	11·0	53·7	4·2	1·25	
	0·75	51·5	37·0	14·5	1·42	1·18	51·5	30·2	21·3	40·85	6·8	1·25	21
	0·50	40	4·7	35·3	0·71	0·78	40	− 4·7	44·7	17·65	9·4	1·25	
Stator	1·0	20·7	0	20·7	2·4	1·65	20·7	− 8·3	29·0	6·2	8·3	1·25	
	0·75	26·7	0	26·7	1·53	1·24	26·7	− 8·9	35·6	8·9	8·9	1·25	20
	0·50	37·1	0	37·1	0·77	0·82	37·1	−10·2	47·3	13·45	10·2	1·25	

C.4 Circular-arc aerofoils

Inlet guide vanes with zero camber and outlet angles

Mean air speed	85·5 ft/sec
Thrust	12·3 lb
Fan speed	41·7 rev/sec
Mass flow	4·64 lb/sec
Fan adiabatic efficiency	0·80
Gear efficiency	0·80
Motor speed	125 rev/sec
Motor power	1·5 b.h.p.

Notation for Table 1 *only*

r		Radius
d		Fan diameter
α_1		Air inlet angle
α_2		Air outlet angle
ϵ	=	$\alpha_1 - \alpha_2$, deflection
α_1'		Blade inlet angle
α_2'		Blade outlet angle
θ	=	$\alpha_1' - \alpha_2'$, camber
ξ		Stagger angle
δ	=	$\alpha_2 - \alpha_2'$, deviation
N		Number of blades
S		Gap
c		Chord, in.
Suffix $_N$		Nominal
Suffix $_A$		Actual

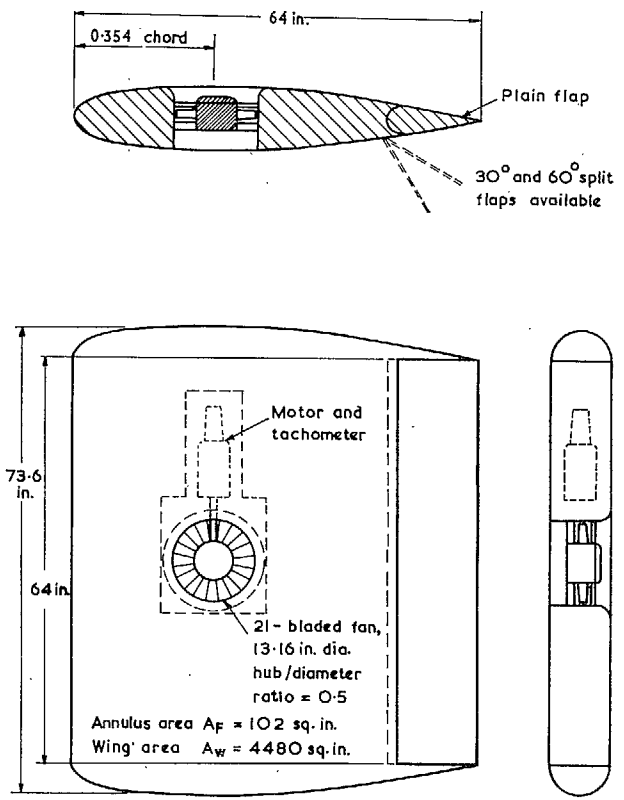

FIG. 1. General arrangement of model.

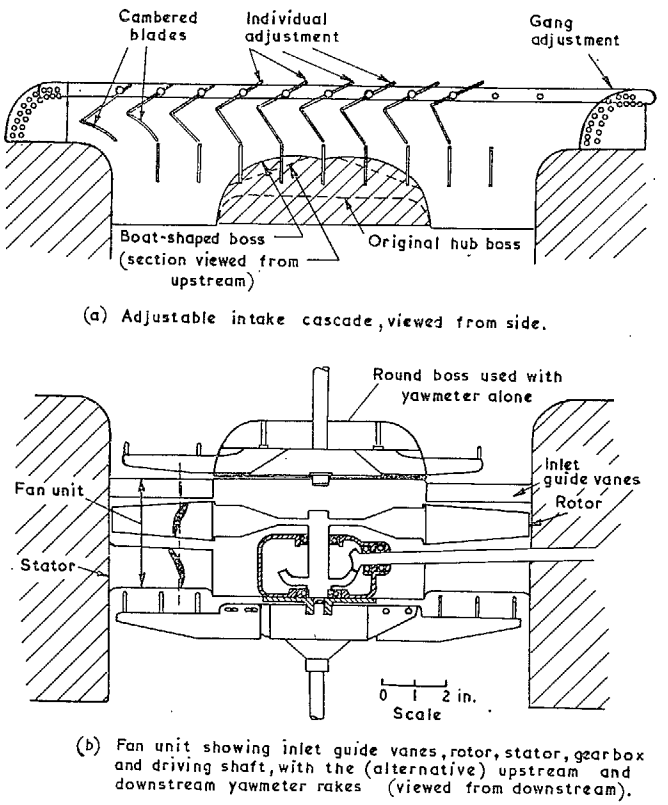

(a) Adjustable intake cascade, viewed from side.

(b) Fan unit showing inlet guide vanes, rotor, stator, gearbox and driving shaft, with the (alternative) upstream and downstream yawmeter rakes (viewed from downstream).

FIG. 2. Details of installation of fan unit, intake cascade and yawmeter rakes.

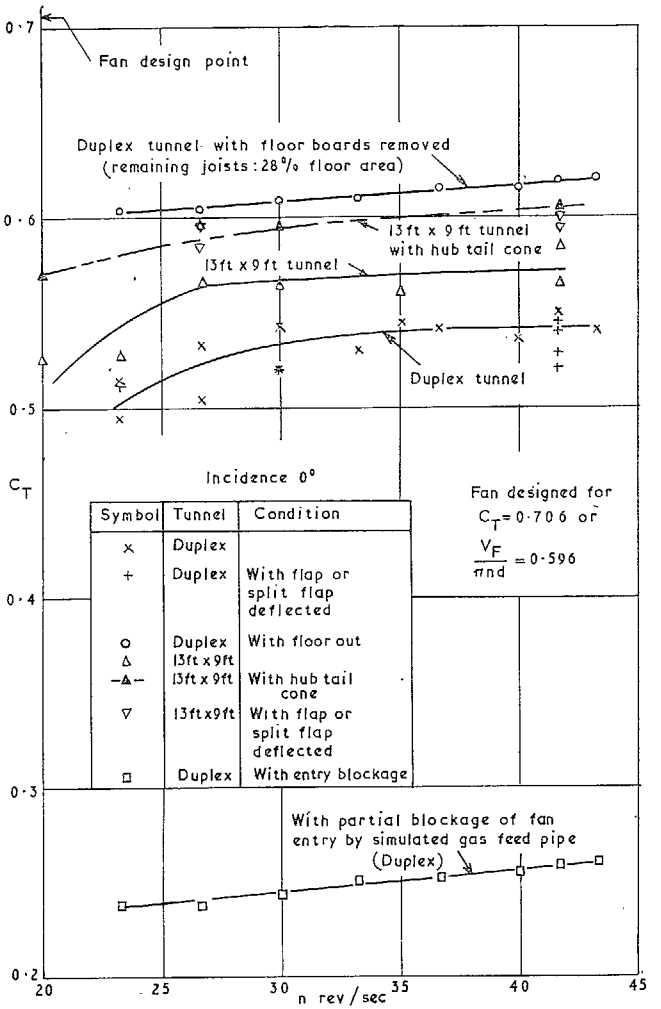

FIG. 3. Scale effect and effect of tunnel constraint and of feed-pipe interference on fan-wing static thrust coefficient.

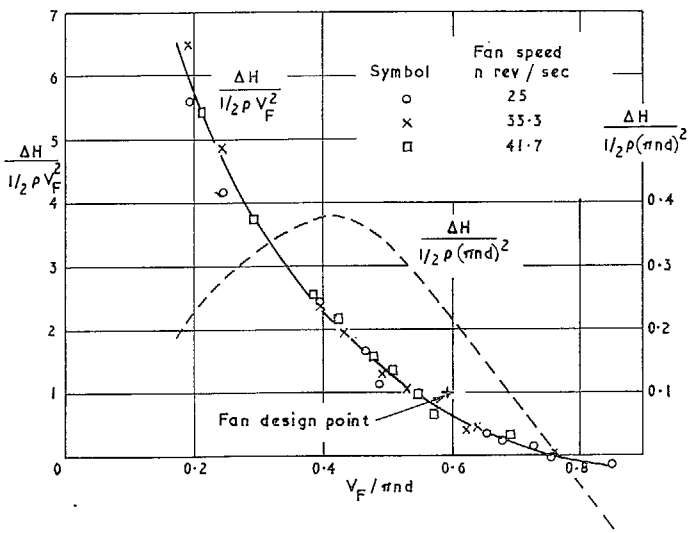

FIG. 4. Total-head rise characteristic of fan (adapted from Ref. 7).

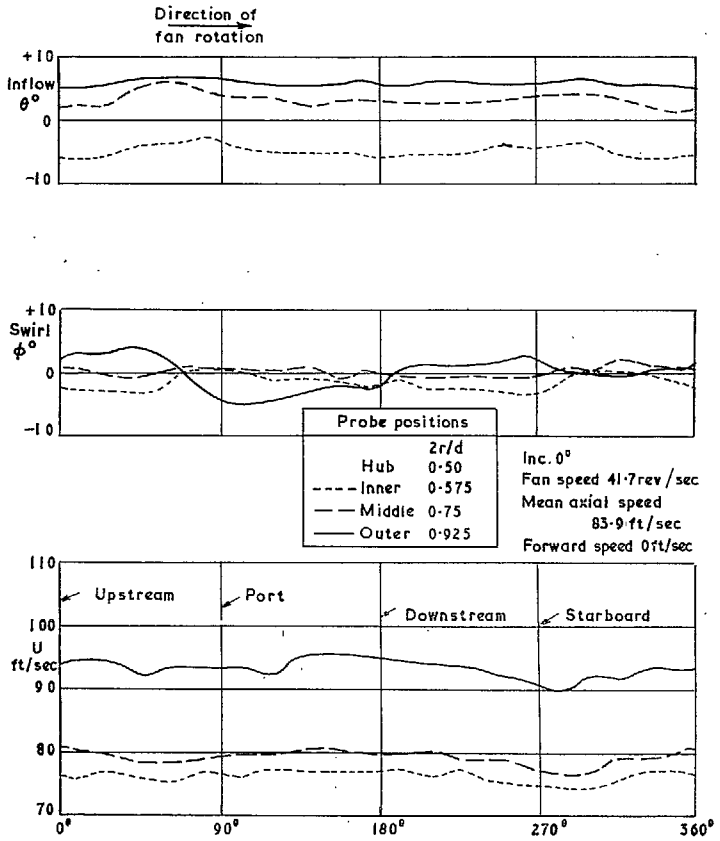

FIG. 5. Upstream circumferential distribution of flow: $V_T/V_F = 0$.

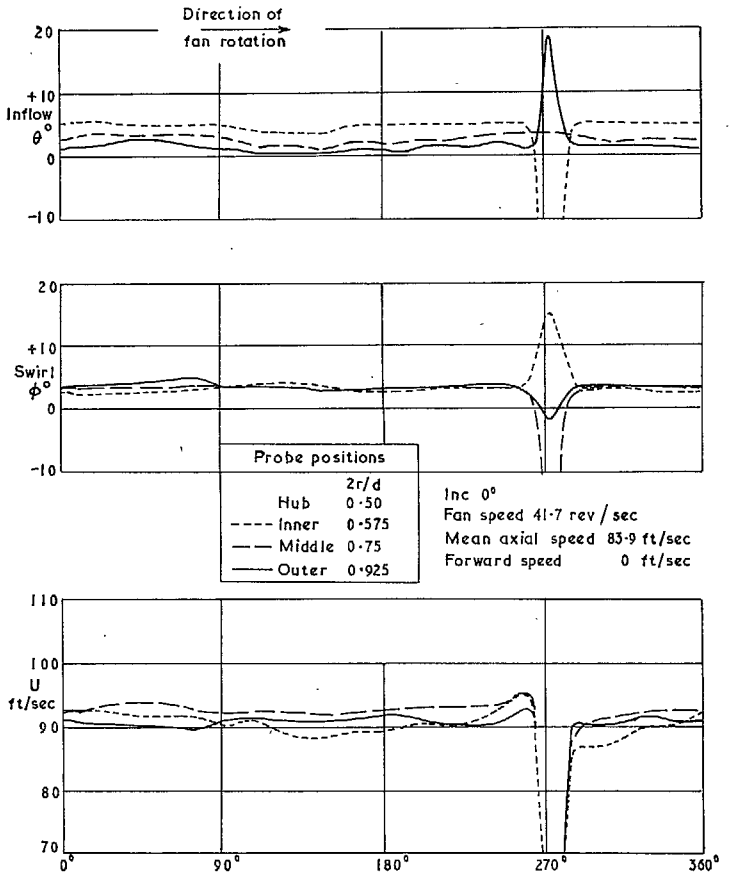

FIG. 6. Downstream circumferential distribution of flow: $V_T/V_F = 0$.

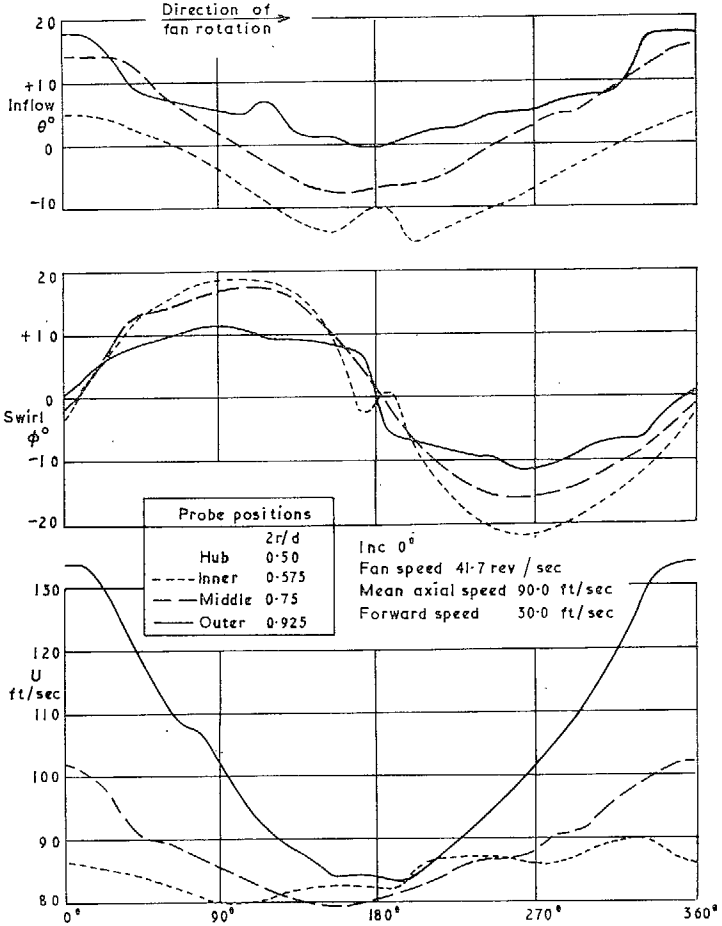

Fig. 7. Upstream circumferential distribution of flow: $V_T/V_F = 0{\cdot}33$.

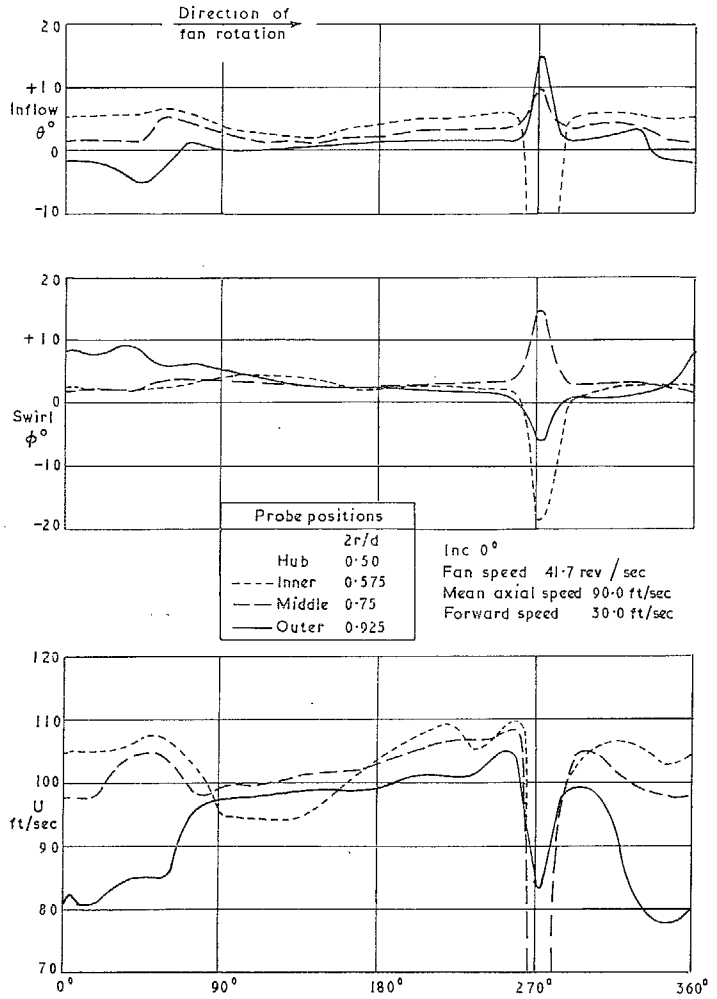

FIG. 8. Downstream circumferential distribution of flow: $V_T/V_F = 0{\cdot}33$.

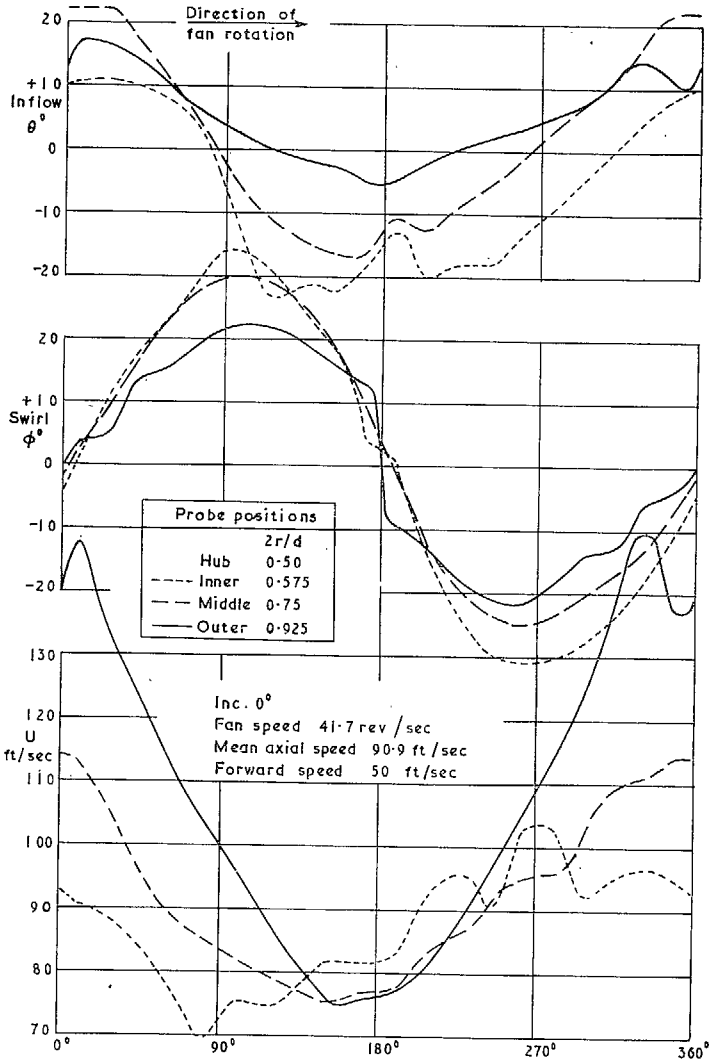

FIG. 9. Upstream circumferential distribution of flow: $V_T/V_F = 0{\cdot}55$.

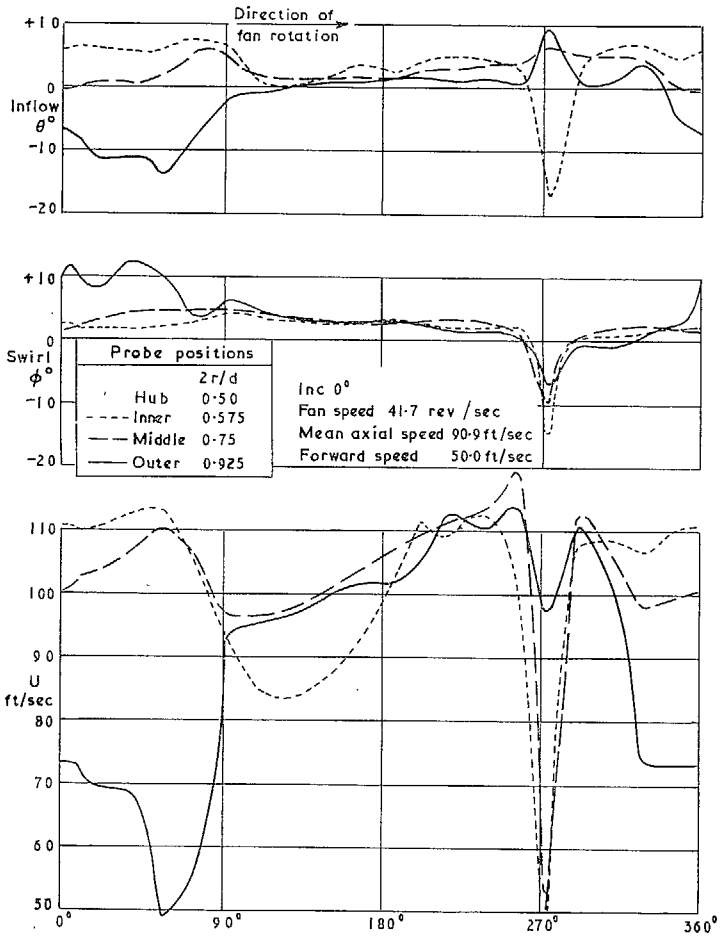

FIG. 10. Downstream circumferential distribution of flow: $V_T/V_F = 0{\cdot}55$.

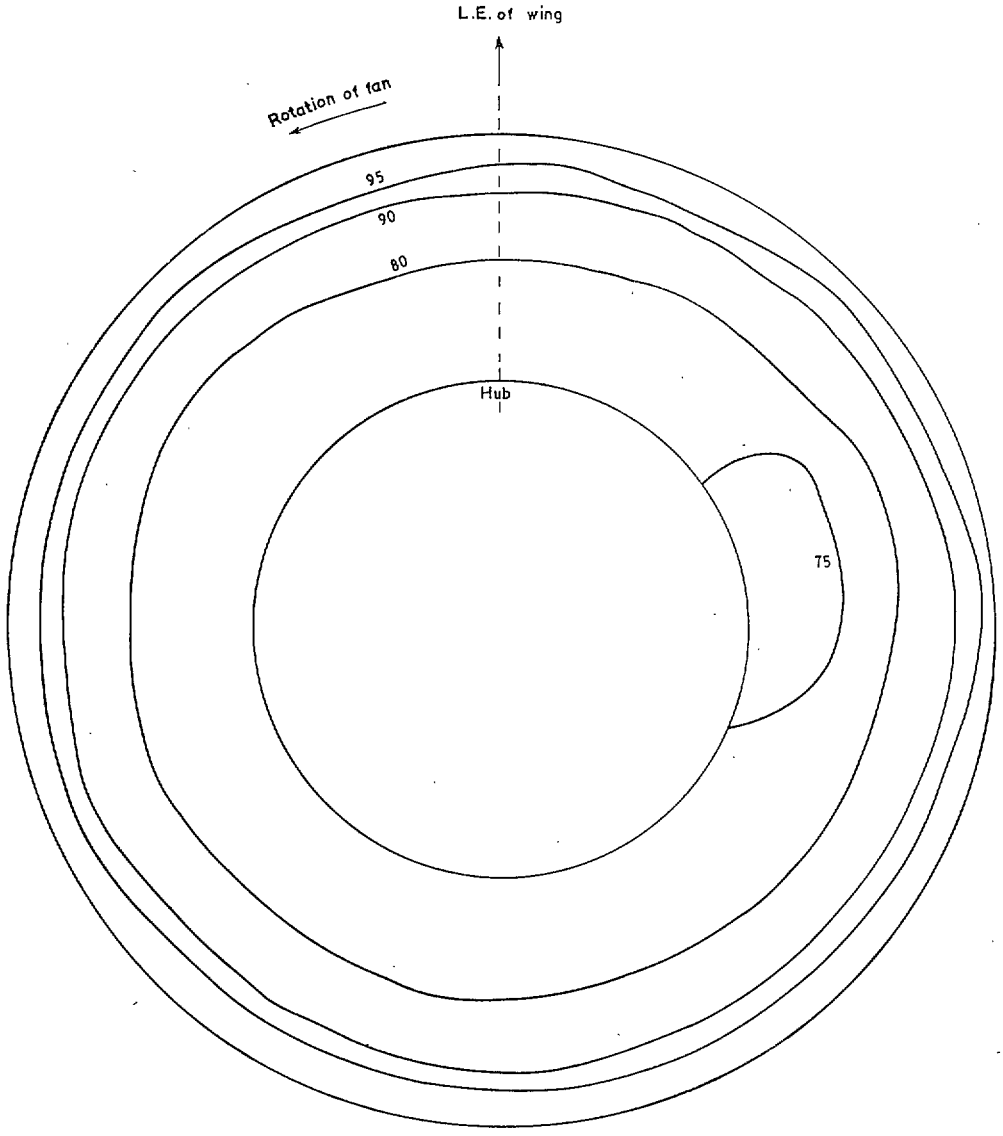

FIG. 11. Equi-velocity contours for flow distribution at fan inlet at 41·7 rev/sec and zero forward speed: $V_T/V_F = 0$. Numbers indicate windspeed in ft/sec. Mean axial speed through fan 83·9 ft/sec.

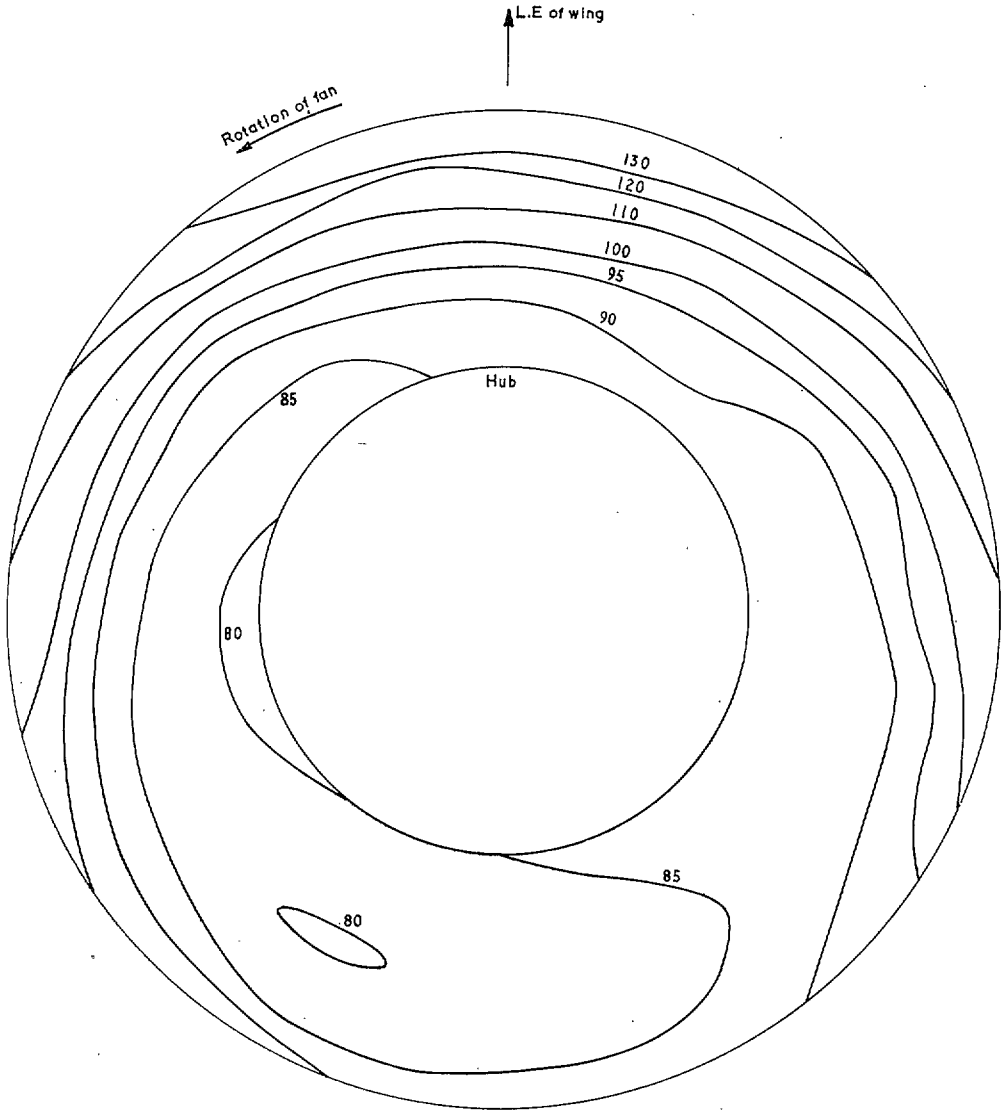

FIG. 12a. Equi-velocity contours for flow distribution at fan inlet at 41·7 rev/sec and 30 ft/sec forward speed: $V_T/V_F = 0{\cdot}33$. Numbers indicate windspeed in ft/sec. Mean axial speed 90 ft/sec.

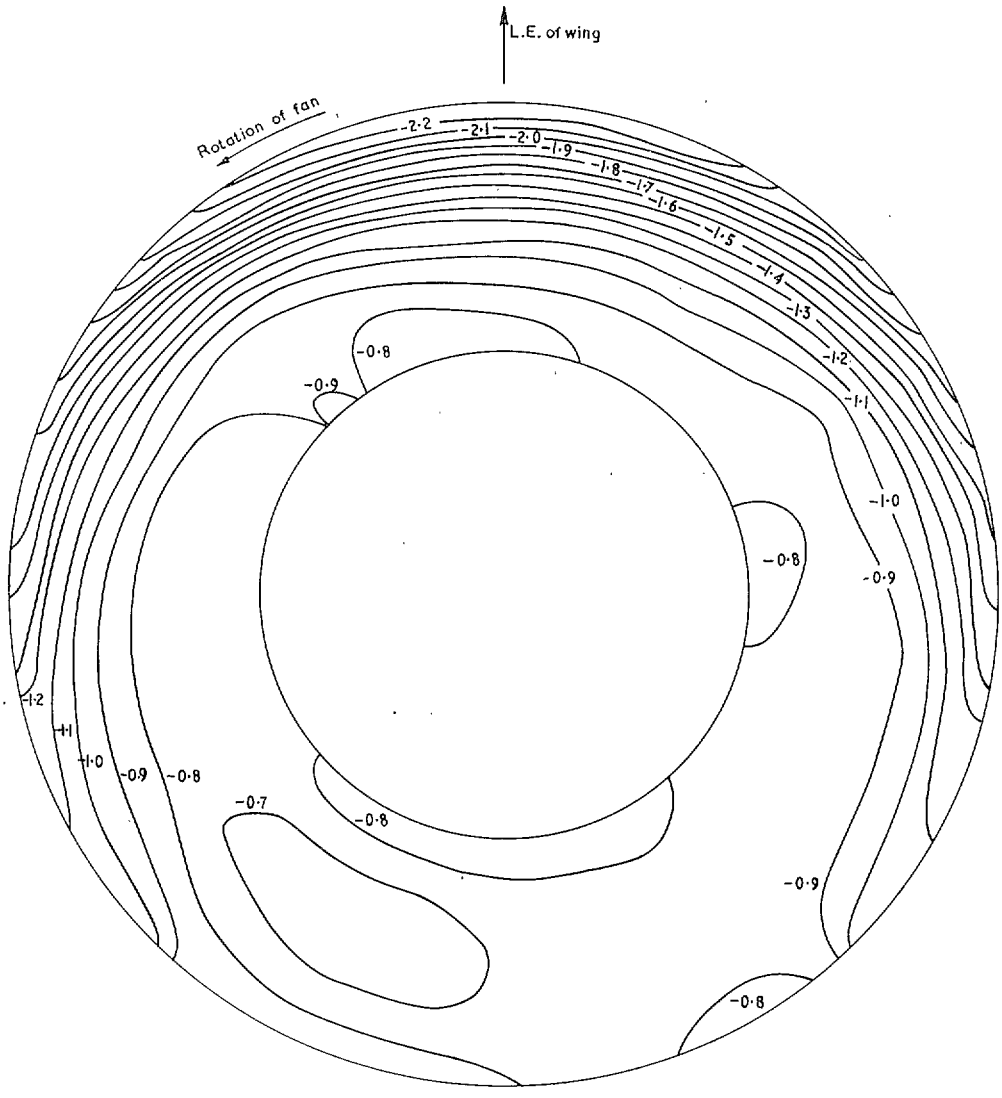

FIG. 12b. Static-pressure contours, $(p - p_T)/\frac{1}{2}\rho V_F^2$, at fan inlet at 41·7 rev/sec and 30 ft/sec forward speed: $V_T/V_F = 0{\cdot}33$.

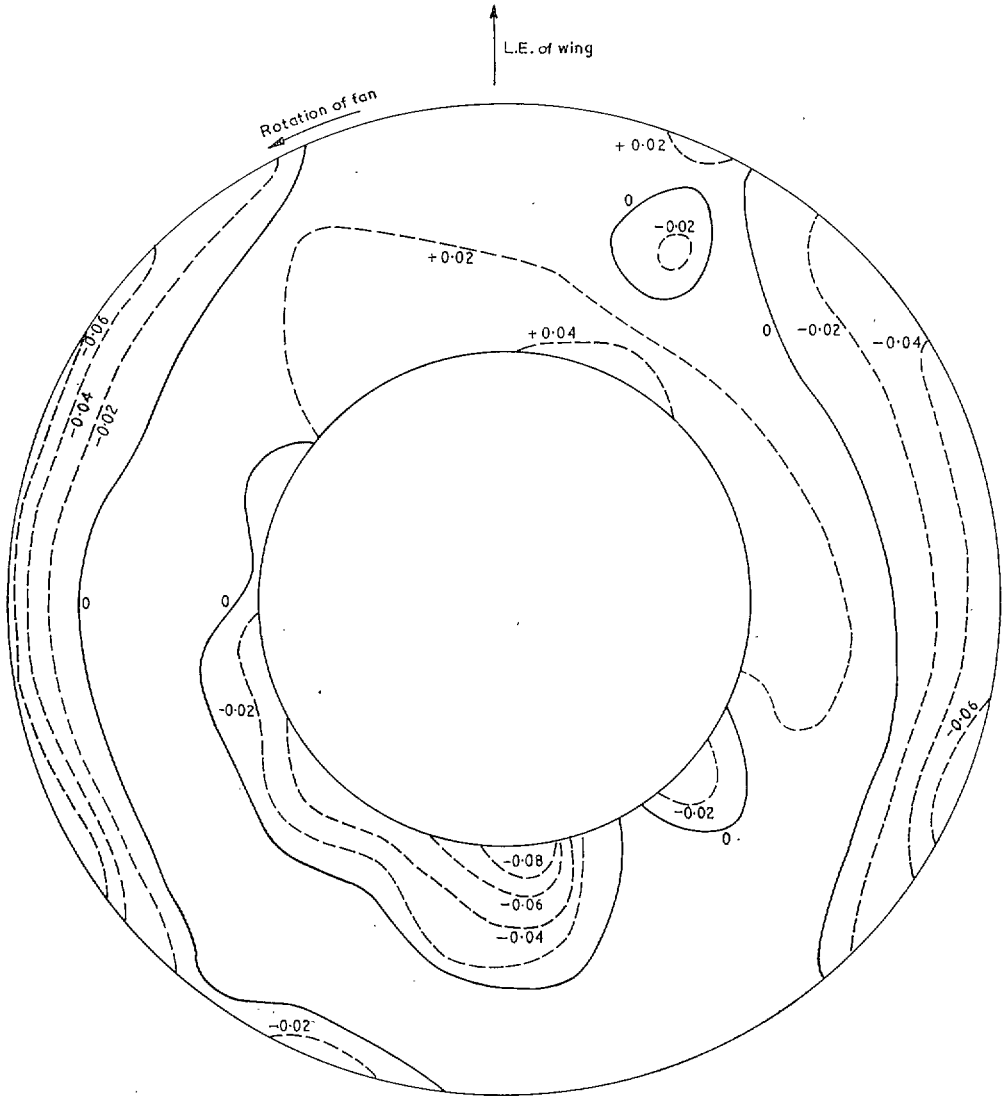

FIG. 12c. Total-head contours, $(H - H_{\text{mean}})/\frac{1}{2}\rho V_F^2$, at fan inlet at 41·7 rev/sec and 30 ft/sec forward speed: $V_T/V_F = 0{\cdot}33$.

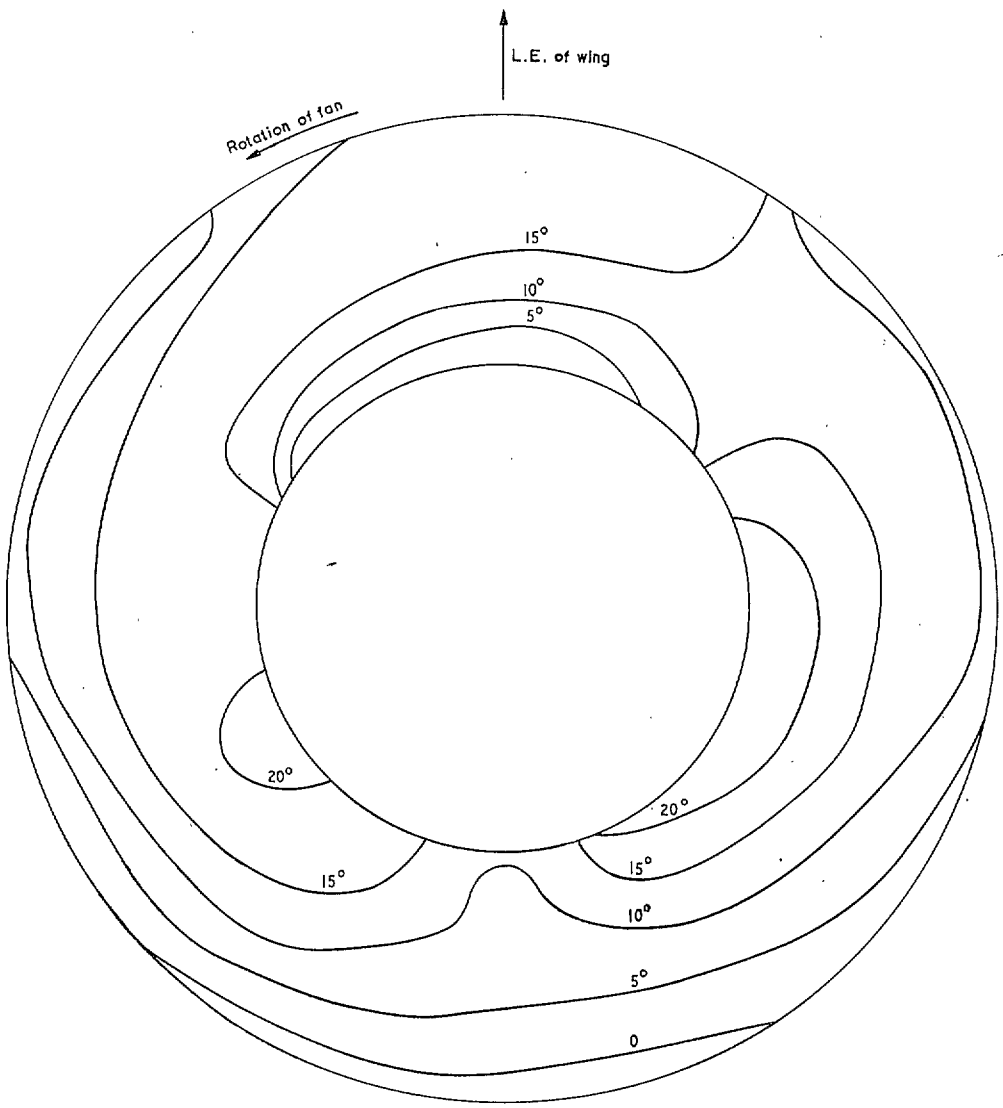

FIG. 12d. Contours of underturning angle, α, at fan inlet at 41·7 rev/sec and 30 ft/sec forward speed: $V_T/V_F = 0{\cdot}33$.

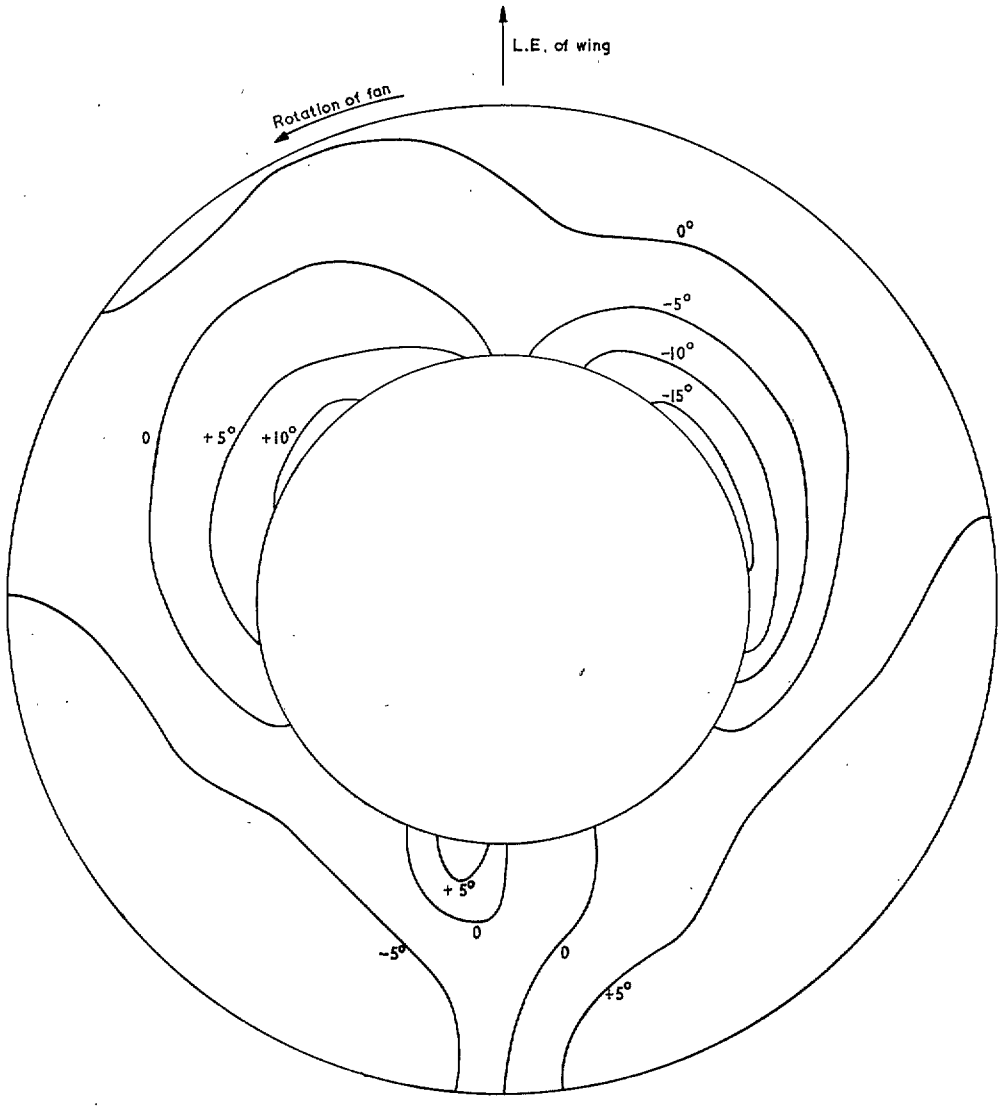

FIG. 12e. Contours of spanwise flow angle, β, at fan inlet at 41·7 rev/sec and 30 ft/sec forward speed: $V_T/V_F = 0{\cdot}33$. Positive β indicates flow to the left.

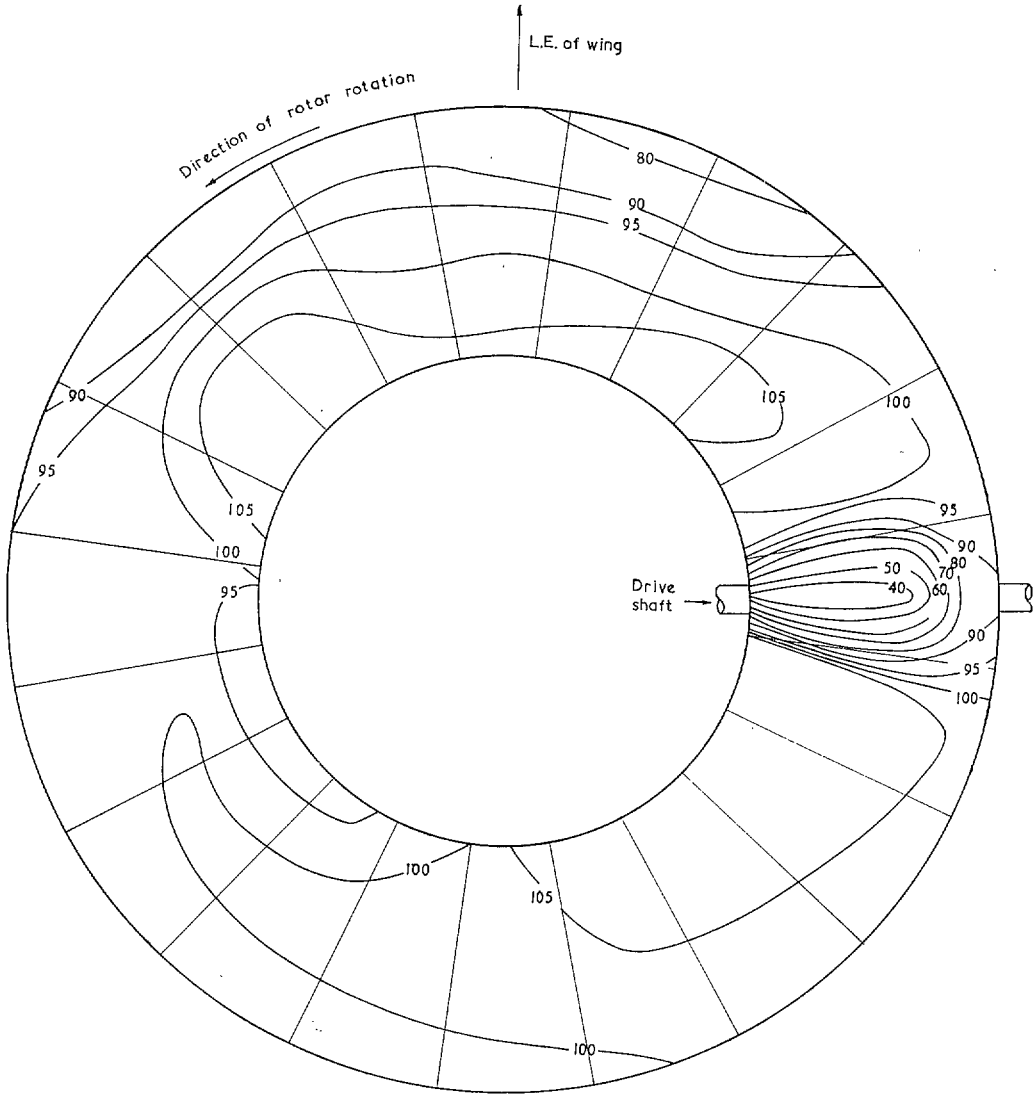

FIG. 13a. Equi-velocity contours for flow distribution at fan exit at 41·7 rev/sec. and 30 ft/sec forward speed: $V_T/V_F = 0{\cdot}33$. Numbers indicate windspeed in ft/sec. Mean axial speed 90 ft/sec.

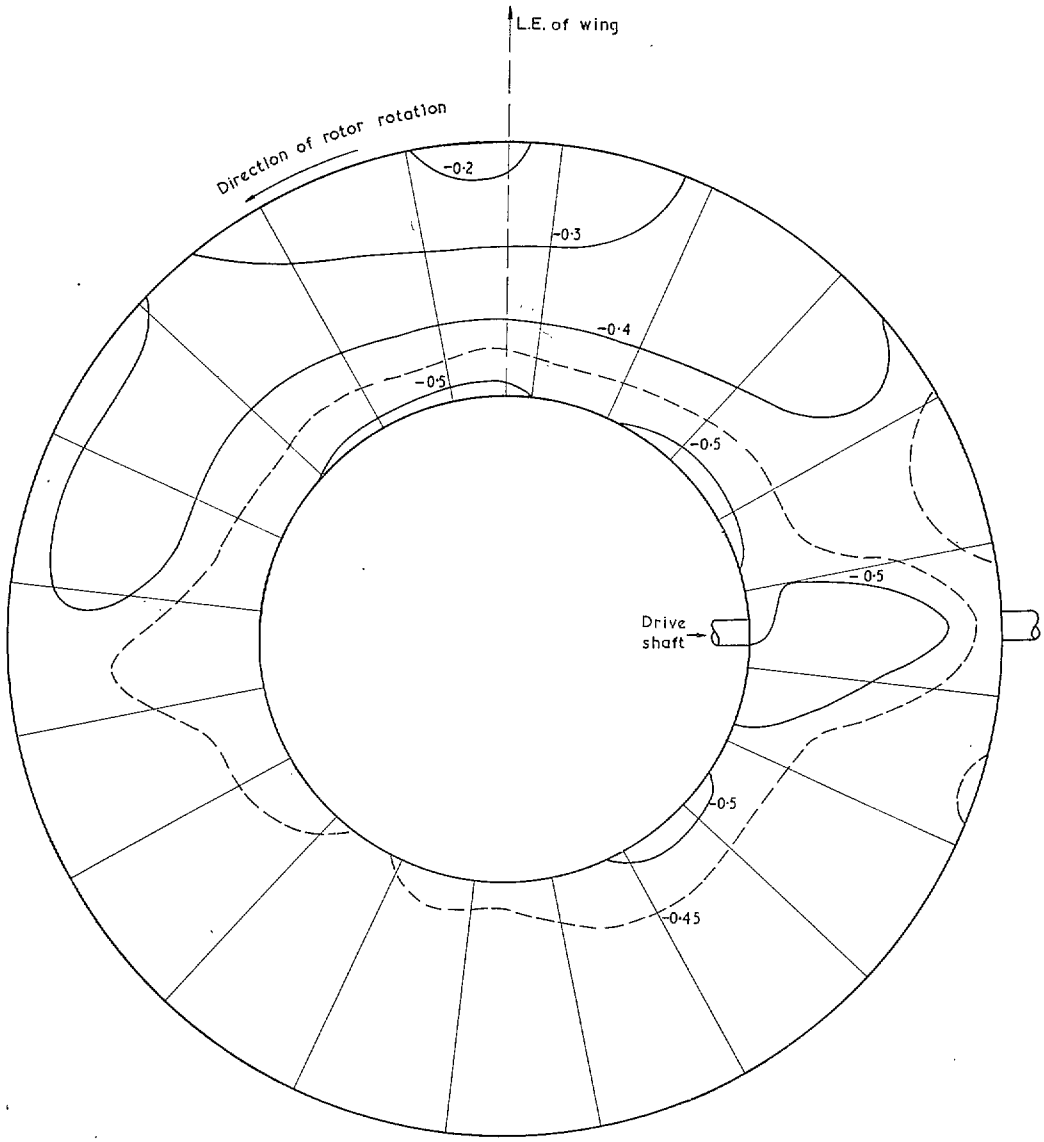

FIG. 13b. Static-pressure contours $(p - p_T)/\frac{1}{2}\rho V_F^2$ at fan exit at 41·7 rev/sec and 30 ft/sec forward speed. $V_T/V_F = 0 \cdot 33$.

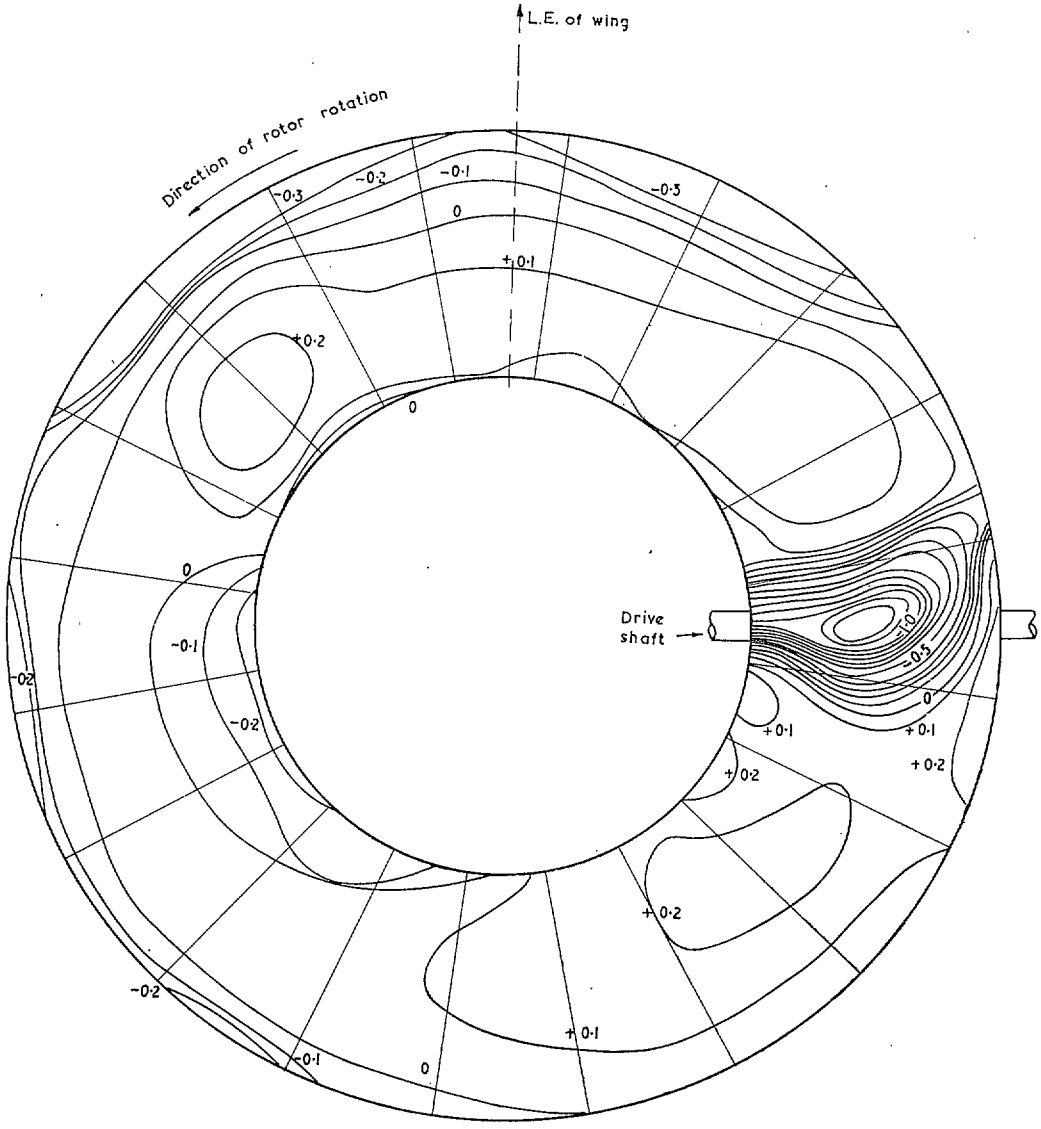

FIG. 13c. Total-head contours, $(H - H_{\text{mean}})/\frac{1}{2}\rho V_F^2$, at fan exit at 41·7 ft/sec and 30 ft/sec forward speed: $V_T/V_F = 0{\cdot}33$.

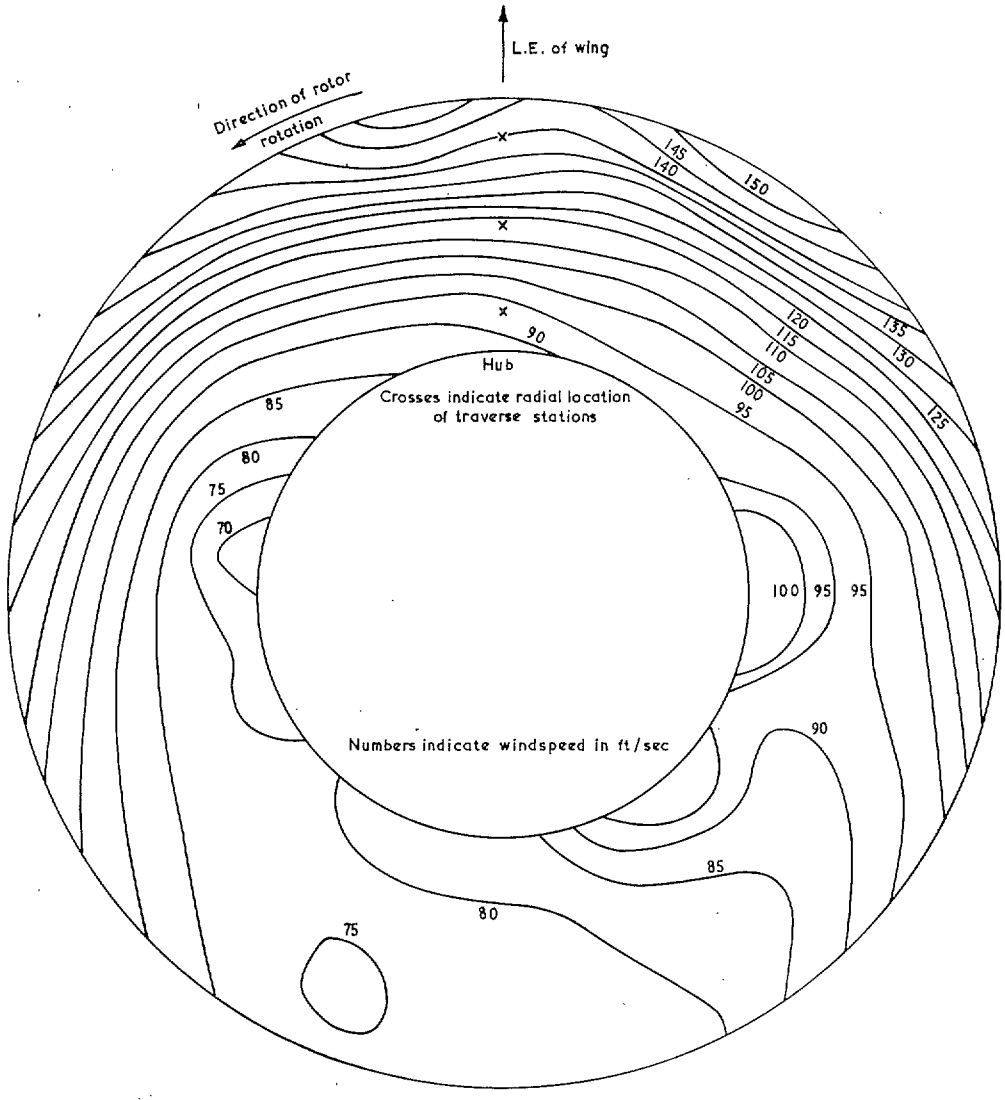

FIG. 14a. Equi-velocity contours for flow distribution at fan inlet at 41·7 rev/sec and 50 ft/sec forward speed: $V_T/V_F = 0{\cdot}55$. Mean axial speed 90·9 ft/sec.

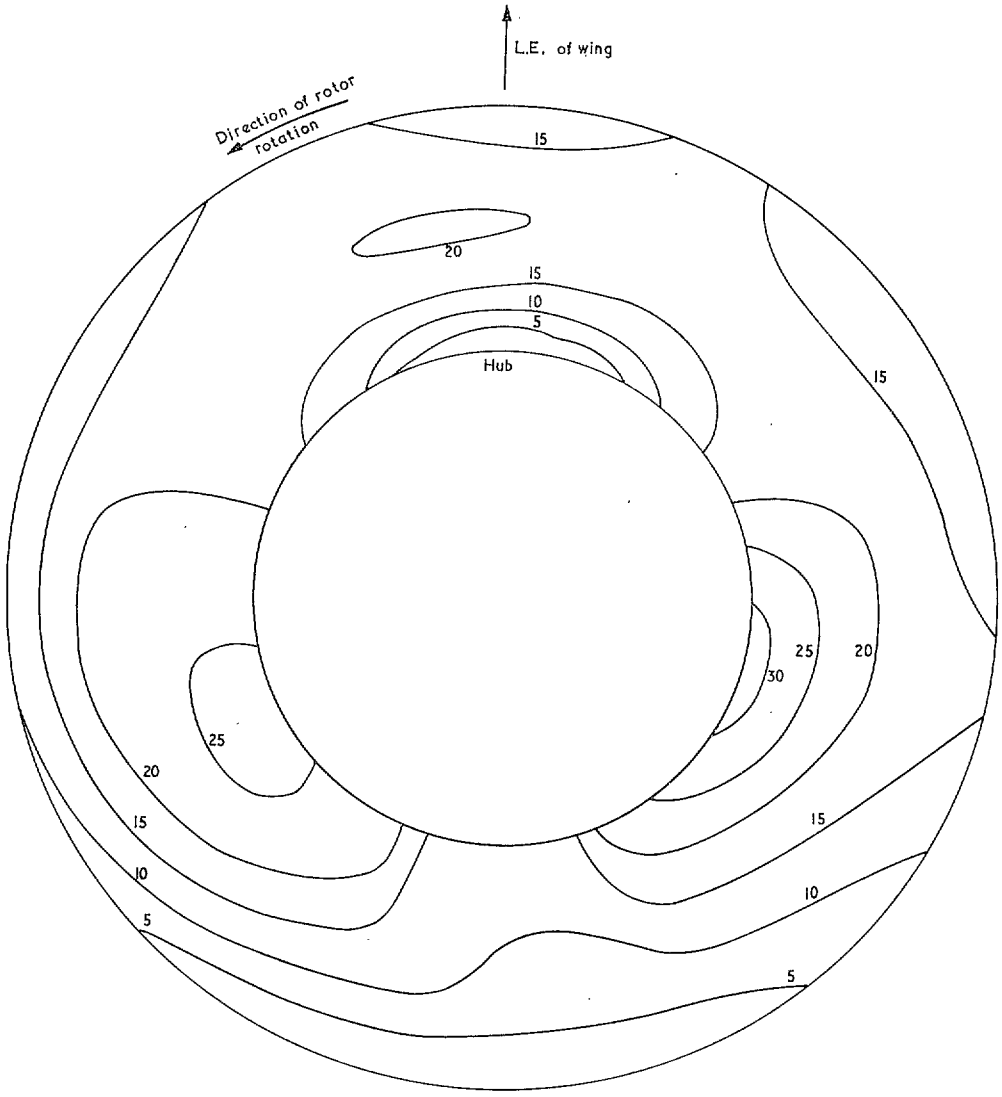

FIG. 14b. Contours of flow underturning angle, α, at fan inlet at 41·7 rev/sec and 50 ft/sec forward speed.

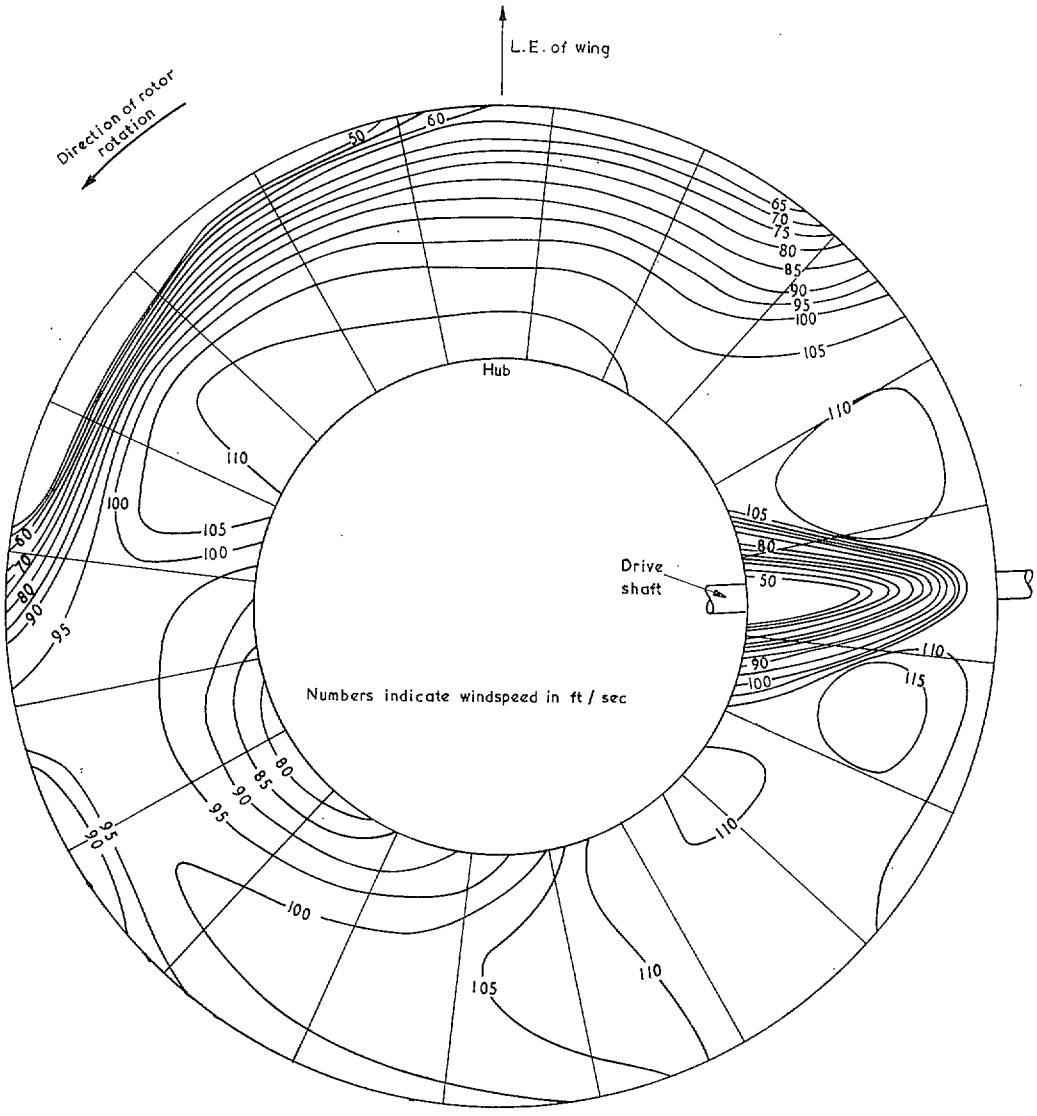

FIG. 15. Equi-velocity contours for flow distribution at fan exit at 41·7 rev/sec and 50 ft/sec forward speed: $V_T/V_F = 0{\cdot}55$. Mean axial speed 90·9 ft/sec.

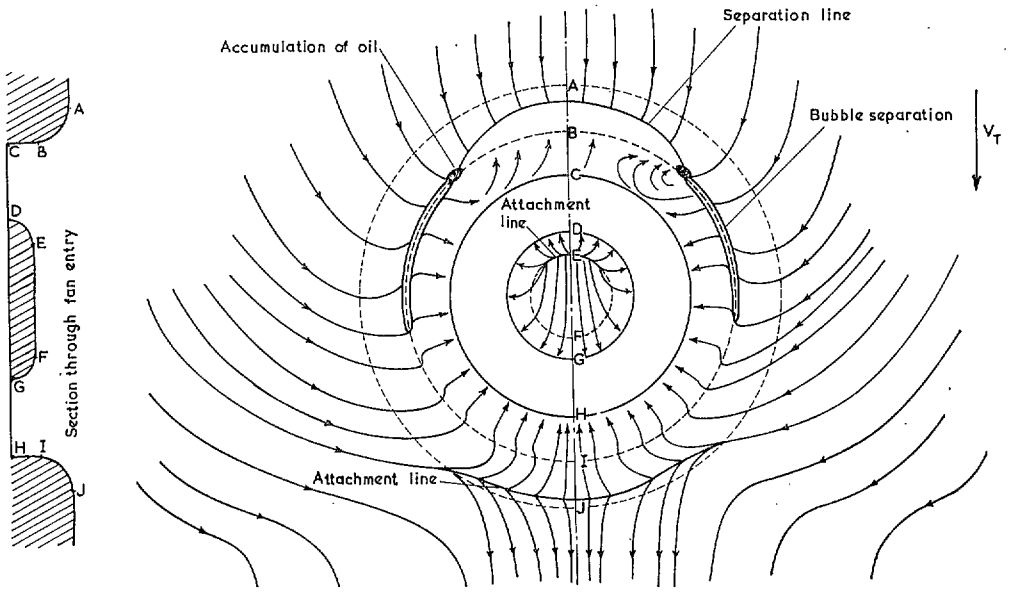

FIG. 16. Oil-flow pattern on the wing and fan entry for $V_T/V_F = 0{\cdot}55$: developed surfaces.

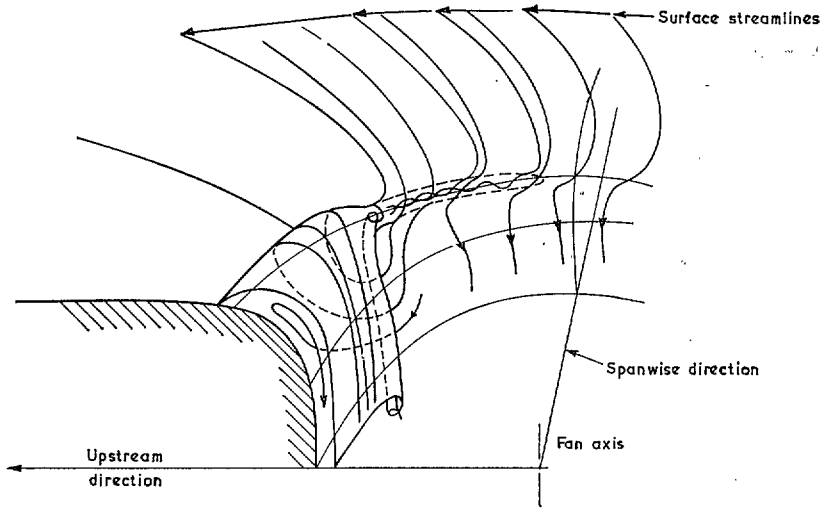

FIG. 17. Sketch indicating short and long bubbles of separation observed at $V_T/V_F = 0{\cdot}55$.

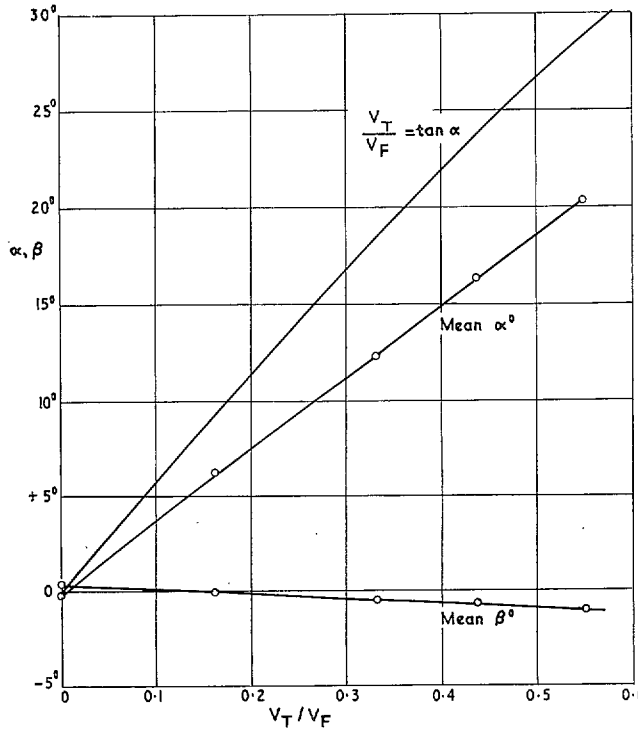

FIG. 18. Variation with forward-speed ratio V_T/V_F of mean underturning ($\alpha°$) and spanwise flow angle ($\beta°$) without entry cascade (+ve β is flow in direction of fan rotation at front of duct).

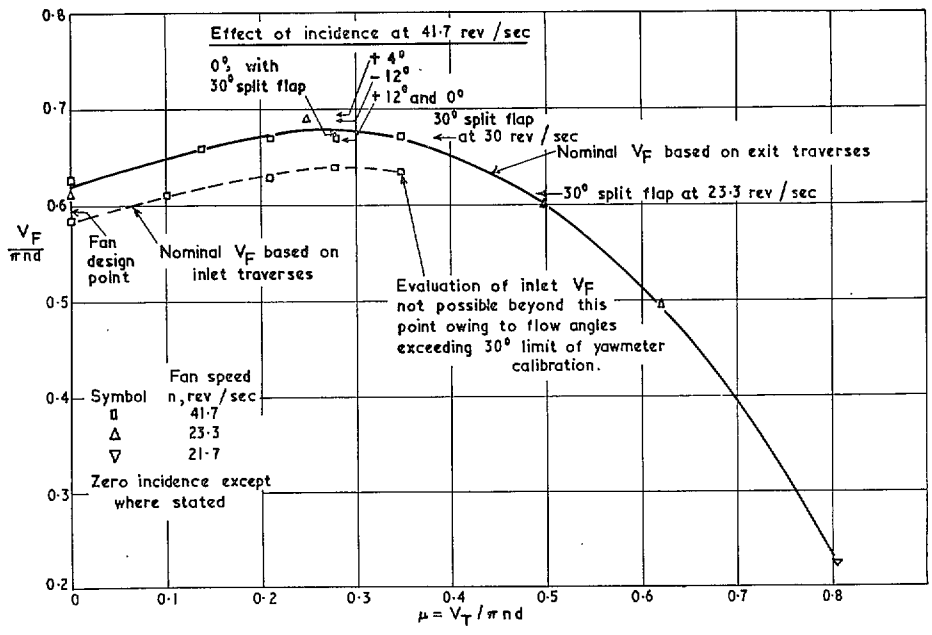

FIG. 19. Effect of forward speed (V_T) on mean flow speed (V_F) through fan with plain circular entry.

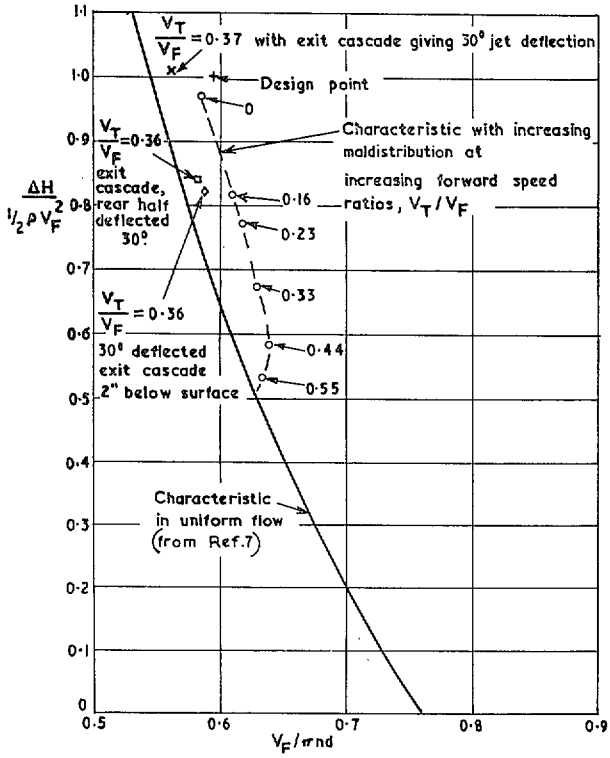

FIG. 20. Effect of maldistribution due to forward speed on total-head rise characteristic of fan.

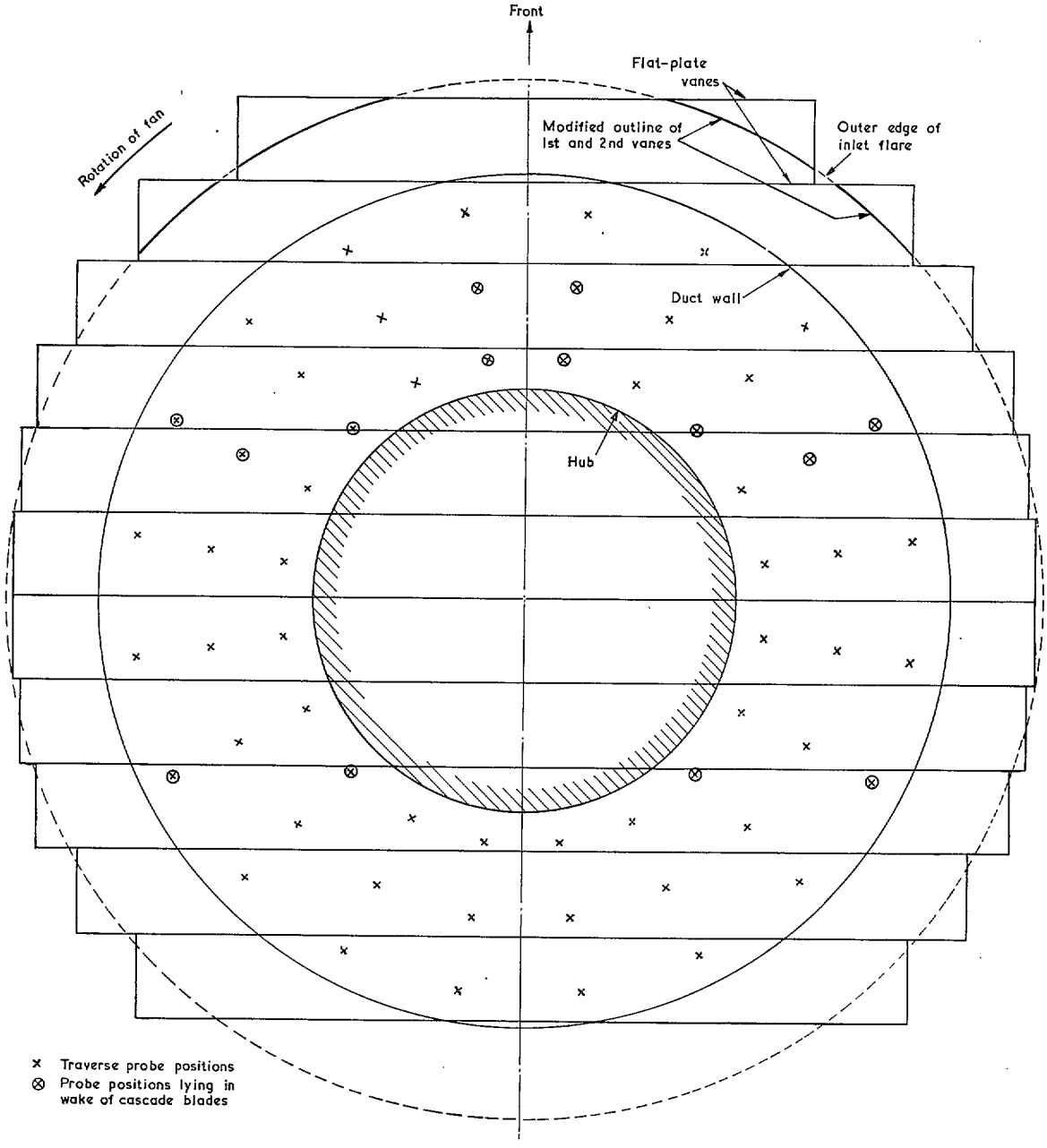

FIG. 21. Plan view of fan duct showing traverse positions and intake cascade vanes in closed positions.

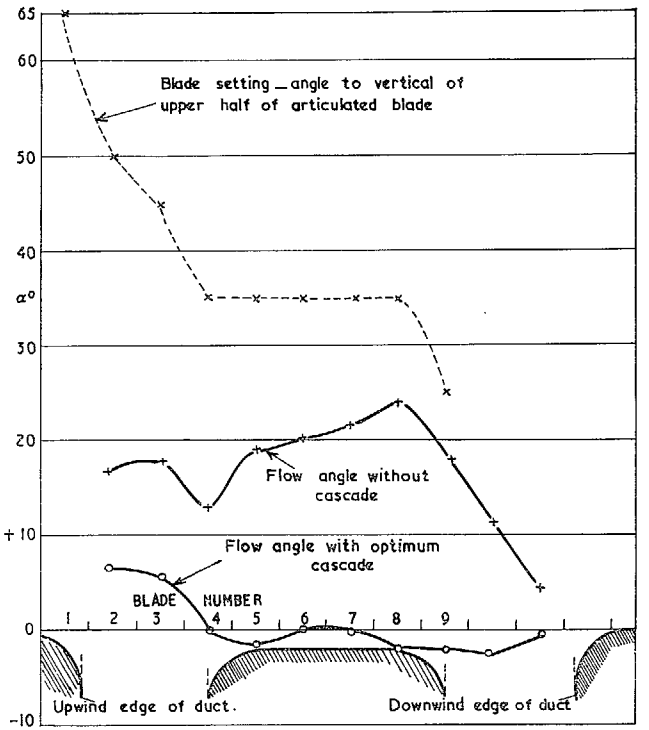

FIG. 22. Mean flow angles below the cascade blades at 41·7 rev/sec fan speed and 40/ft sec tunnel speed ($V_T/V_F \approx 0{\cdot}44$) without cascade, and with optimum setting of blades.

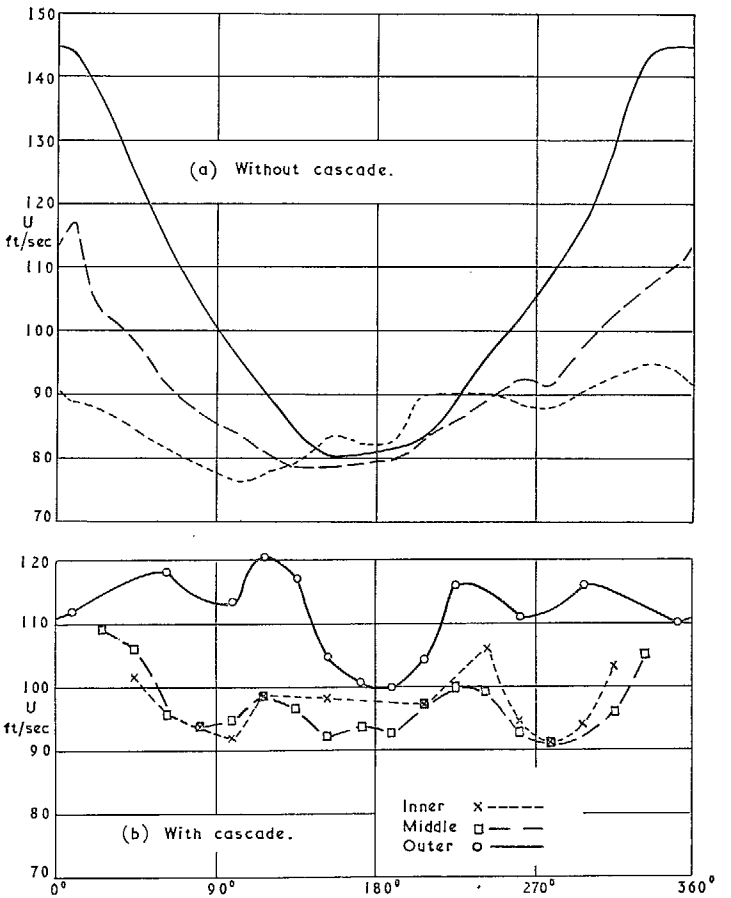

FIG. 23. Upstream circumferential distribution of flow velocity at 40 ft/sec forward speed (V_T/V_F approximately 0·44) found (*a*) without, and (*b*) with optimum cascade.

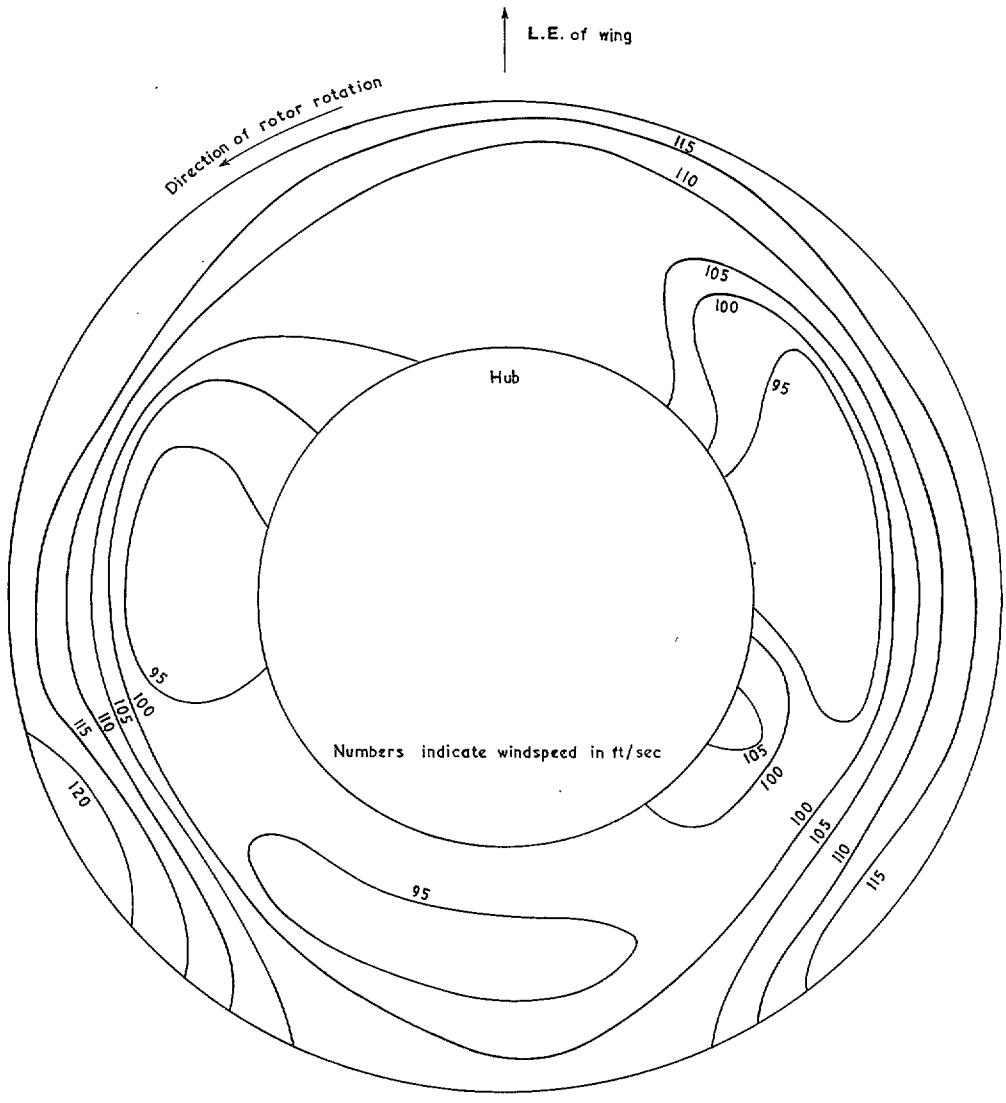

FIG. 24. Equi-velocity contours for flow distribution at fan inlet at 41·7 rev/sec and 40 ft/sec forward speed with optimum setting of inlet cascade fitted to upper surface of wing.

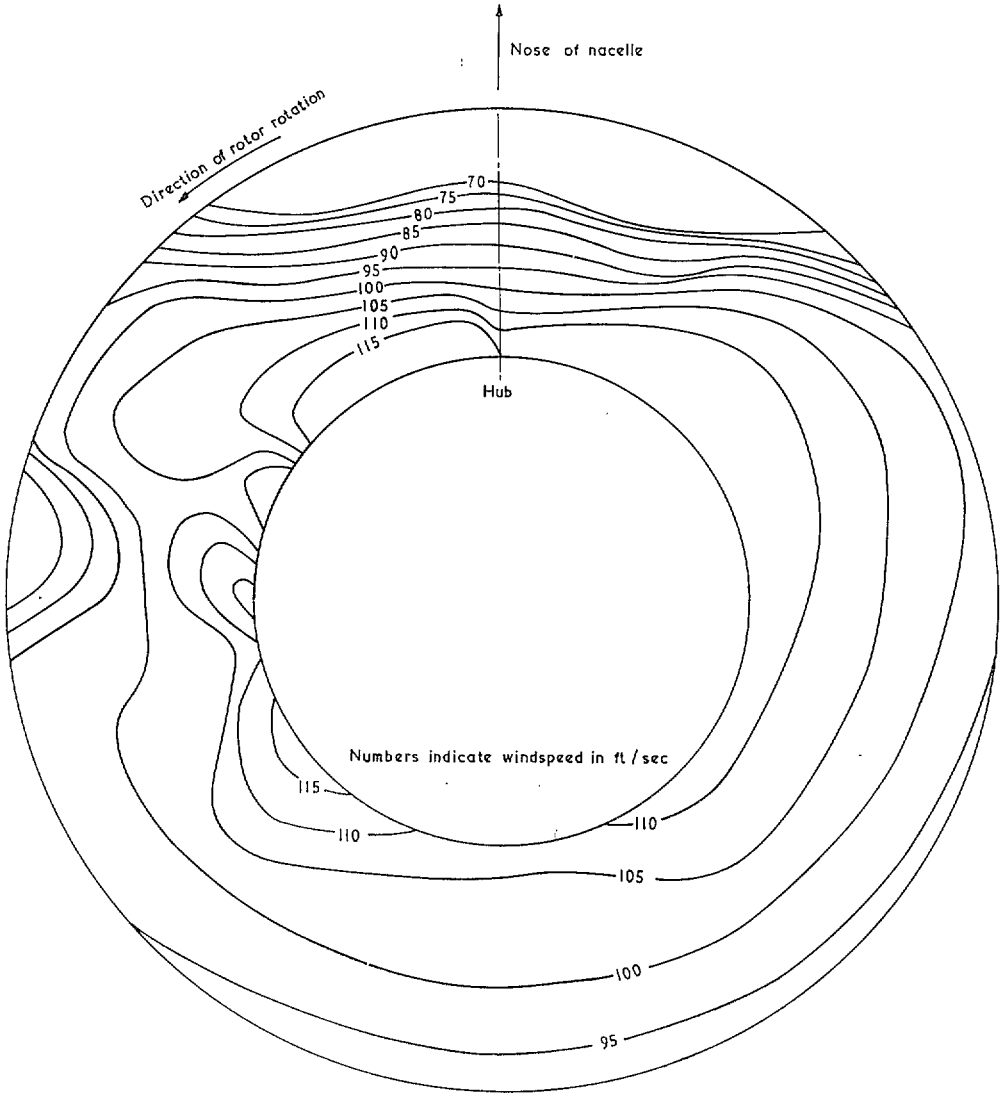

FIG. 25a. Equi-velocity contours for flow distribution at front fan inlet. Both fans at 41·7 rev/sec and 50 ft/sec forward speed. Traverse plane 1 in. ahead of fan inlet guide vanes.

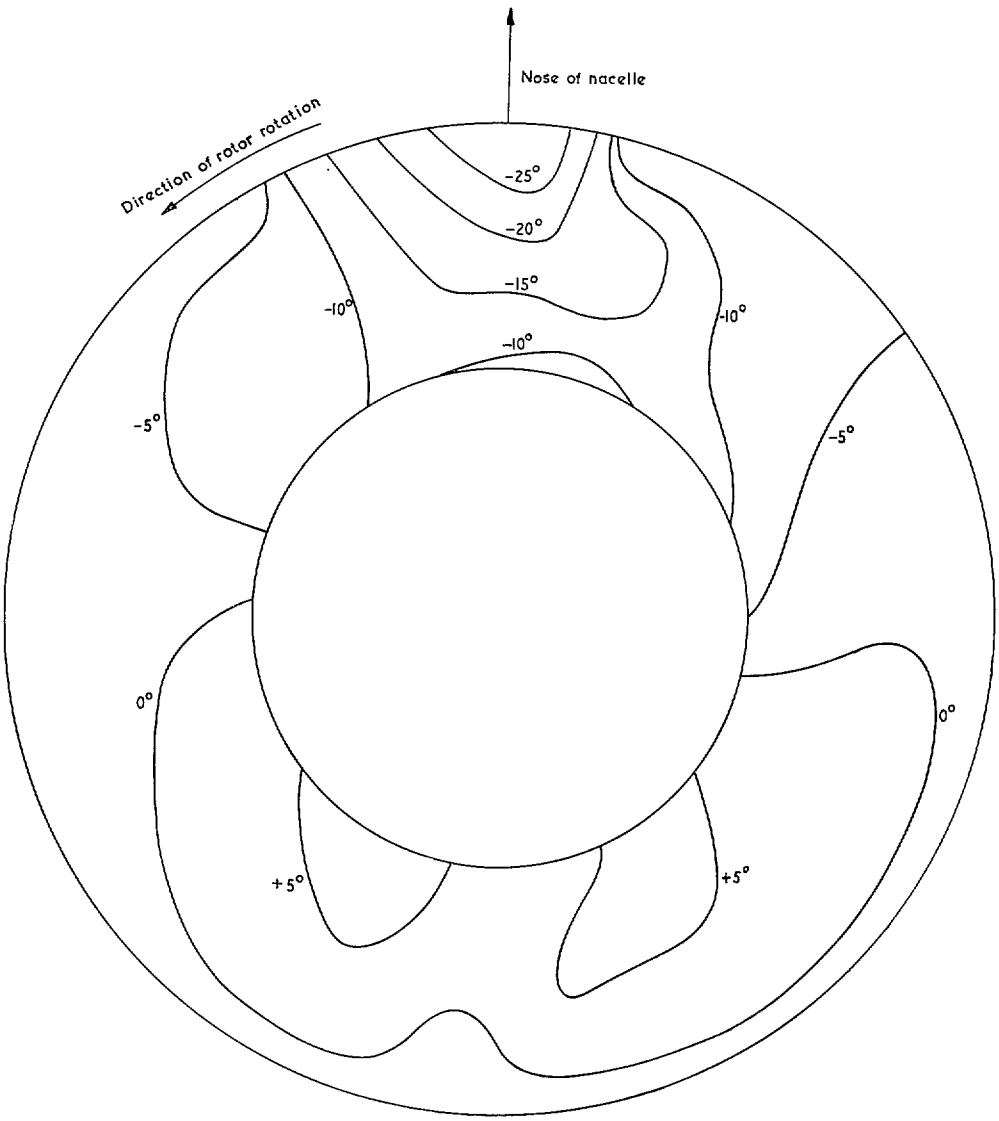

FIG. 25b. Contours of flow underturning angle, α, at front fan inlet. Both fans at 41·7 rev/sec and 50 ft/sec forward speed.

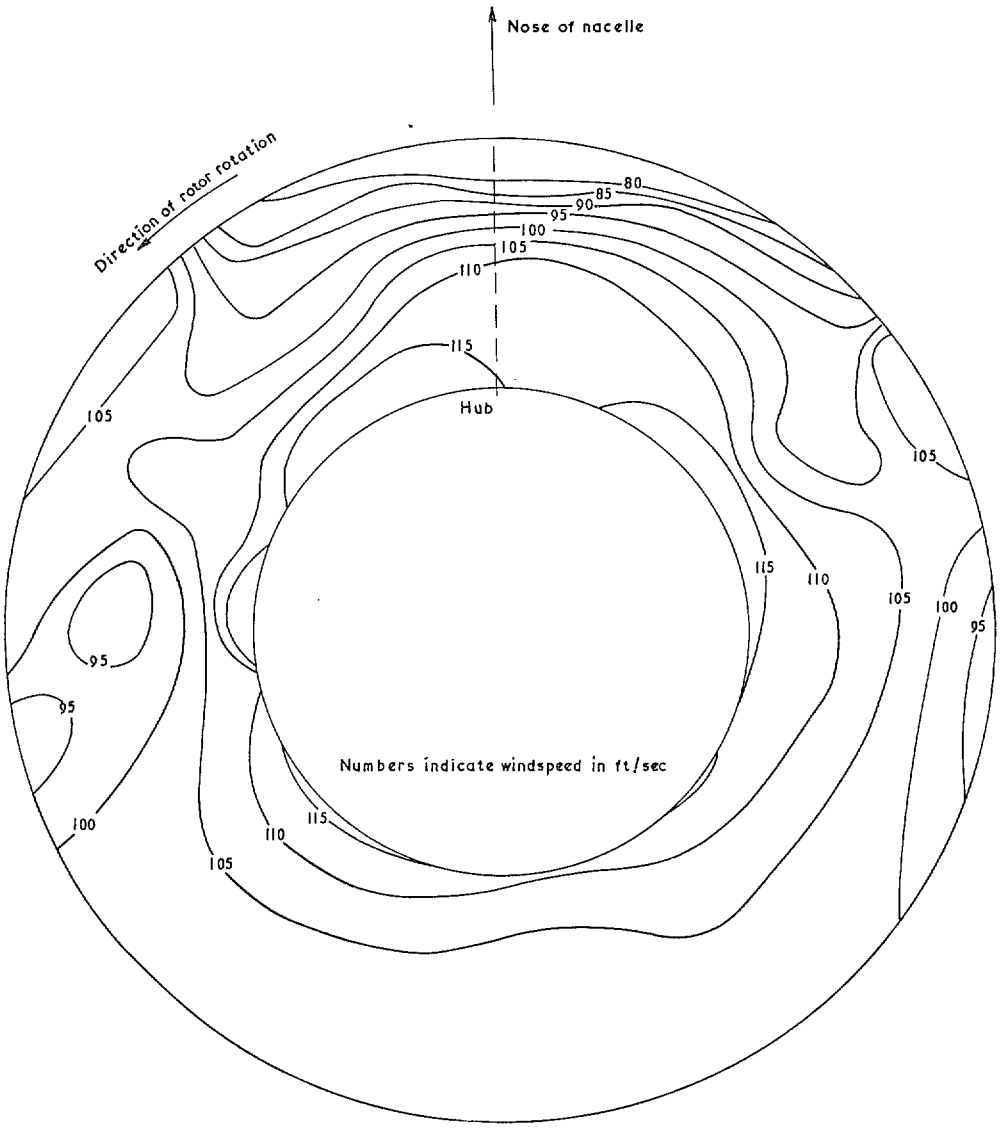

FIG. 26a. Equi-velocity contours for flow distribution at front fan inlet. Both fans at 41·7 rev/sec with half-ring slats fitted. 50 ft/sec forward speed.

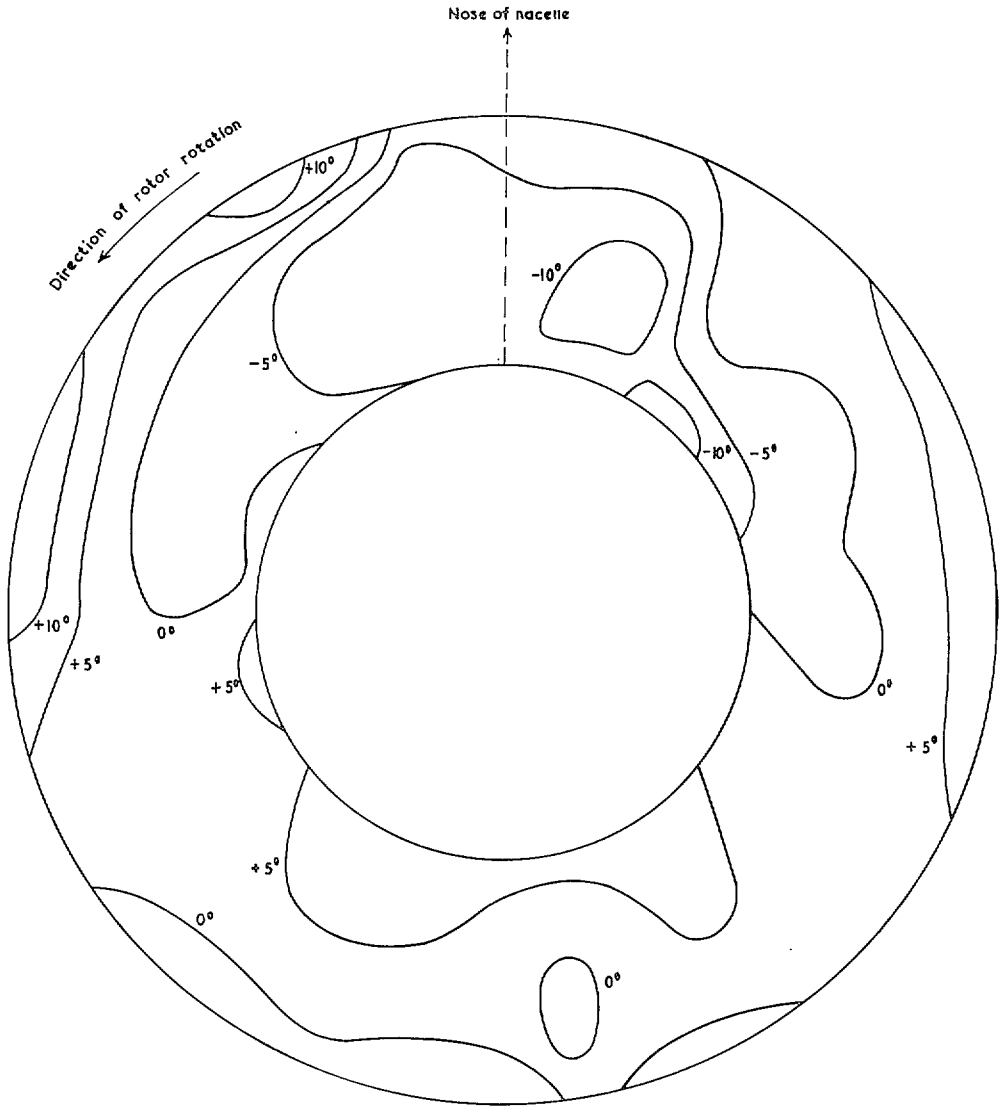

FIG. 26b. Contours of flow underturning angle, α, at front fan inlet. Both fans at 41·7 rev/sec with half-ring slats fitted. 50 ft/sec forward speed.

(90630) Wt. 66/2301 K.5 12/64 Hw.

Publications of the Aeronautical Research Council

ANNUAL TECHNICAL REPORTS OF THE AERONAUTICAL RESEARCH COUNCIL (BOUND VOLUMES)

1942 Vol. I. Aero and Hydrodynamics, Aerofoils, Airscrews, Engines. 75*s.* (post 2*s.* 9*d.*)
Vol. II. Noise, Parachutes, Stability and Control, Structures, Vibration, Wind Tunnels. 47*s.* 6*d.* (post 2*s.* 3*d.*)

1943 Vol. I. Aerodynamics, Aerofoils, Airscrews. 80*s.* (post 2*s.* 6*d.*)
Vol. II. Engines, Flutter, Materials, Parachutes, Performance, Stability and Control, Structures. 90*s.* (post 2*s.* 9*d.*)

1944 Vol. I. Aero and Hydrodynamics, Aerofoils, Aircraft, Airscrews, Controls. 84*s.* (post 3*s.*)
Vol. II. Flutter and Vibration, Materials, Miscellaneous, Navigation, Parachutes, Performance, Plates and Panels, Stability, Structures, Test Equipment, Wind Tunnels. 84*s.* (post 3*s.*)

1945 Vol. I. Aero and Hydrodynamics, Aerofoils. 130*s.* (post 3*s.* 6*d.*)
Vol. II. Aircraft, Airscrews, Controls. 130*s.* (post 3*s.* 6*d.*)
Vol. III. Flutter and Vibration, Instruments, Miscellaneous, Parachutes, Plates and Panels, Propulsion. 130*s.* (post 3*s.* 3*d.*)
Vol. IV. Stability, Structures, Wind Tunnels, Wind Tunnel Technique. 130*s.* (post 3*s.* 3*d.*)

1946 Vol. I. Accidents, Aerodynamics, Aerofoils and Hydrofoils. 168*s.* (post 3*s.* 9*d.*)
Vol. II. Airscrews, Cabin Cooling, Chemical Hazards, Controls, Flames, Flutter, Helicopters, Instruments and Instrumentation, Interference, Jets, Miscellaneous, Parachutes. 168*s.* (post 3*s.* 3*d.*)
Vol. III. Performance, Propulsion, Seaplanes, Stability, Structures, Wind Tunnels. 168*s.* (post 3*s.* 6*d.*)

1947 Vol. I. Aerodynamics, Aerofoils, Aircraft. 168*s.* (post 3*s.* 9*d.*)
Vol. II. Airscrews and Rotors, Controls, Flutter, Materials, Miscellaneous, Parachutes, Propulsion, Seaplanes, Stability, Structures, Take-off and Landing. 168*s.* (post 3*s.* 9*d.*)

1948 Vol. I. Aerodynamics, Aerofoils, Aircraft, Airscrews, Controls, Flutter and Vibration, Helicopters, Instruments, Propulsion, Seaplane, Stability, Structures, Wind Tunnels. 130*s.* (post 3*s.* 3*d.*)
Vol. II. Aerodynamics, Aerofoils, Aircraft, Airscrews, Controls, Flutter and Vibration, Helicopters, Instruments, Propulsion, Seaplane, Stability, Structures, Wind Tunnels. 110*s.* (post 3*s.* 3*d.*)

Special Volumes

Vol. I. Aero and Hydrodynamics, Aerofoils, Controls, Flutter, Kites, Parachutes, Performance, Propulsion, Stability. 126*s.* (post 3*s.*)
Vol. II. Aero and Hydrodynamics, Aerofoils, Airscrews, Controls, Flutter, Materials, Miscellaneous, Parachutes, Propulsion, Stability, Structures. 147*s.* (post 3*s.*)
Vol. III. Aero and Hydrodynamics, Aerofoils, Airscrews, Controls, Flutter, Kites, Miscellaneous, Parachutes, Propulsion, Seaplanes, Stability, Structures, Test Equipment. 189*s.* (post 3*s.* 9*d.*)

Reviews of the Aeronautical Research Council

1939–48 3*s.* (post 6*d.*) 1949–54 5*s.* (post 5*d.*)

Index to all Reports and Memoranda published in the Annual Technical Reports

1909–1947 R. & M. 2600 (out of print)

Indexes to the Reports and Memoranda of the Aeronautical Research Council

Between Nos. 2351–2449	R. & M. No. 2450	2*s.* (post 3*d.*)
Between Nos. 2451–2549	R. & M. No. 2550	2*s.* 6*d.* (post 3*d.*)
Between Nos. 2551–2649	R. & M. No. 2650	2*s.* 6*d.* (post 3*d.*)
Between Nos. 2651–2749	R. & M. No. 2750	2*s.* 6*d.* (post 3*d.*)
Between Nos. 2751–2849	R. & M. No. 2850	2*s.* 6*d.* (post 3*d.*)
Between Nos. 2851–2949	R. & M. No. 2950	3*s.* (post 3*d.*)
Between Nos. 2951–3049	R. & M. No. 3050	3*s.* 6*d.* (post 3*d.*)
Between Nos. 3051–3149	R. & M. No. 3150	3*s.* 6*d.* (post 3*d.*)

HER MAJESTY'S STATIONERY OFFICE

from the addresses overleaf

Printed and published by
HER MAJESTY'S STATIONERY OFFICE

To be purchased from
York House, Kingsway, London W.C.2
423 Oxford Street, London W.1
13A Castle Street, Edinburgh 2
109 St. Mary Street, Cardiff
39 King Street, Manchester 2
50 Fairfax Street, Bristol 1
35 Smallbrook, Ringway, Birmingham 5
80 Chichester Street, Belfast 1
or through any bookseller

Printed in England

S.O. Code No. 23-3388